A DETAILED STUDY OF TELESEISMIC P-WAVE TRAVEL TIME RESIDUALS AT AHMADU BELLO UNIVERSITY ZARIA SEISMIC STATION

BY

ADETOLA SUNDAY ONIKU

A RESEARCH WORK SUBMITTED TO THE DEPARTMENT OF PHYSICS AHMADU BELLO UNIVERSITY, ZARIA IN PARTIAL FULFILLMENT FOR THE AWARD OF M. Sc. DEGREE IN APPLIED GEOPHYSICS

AUGUST, 1999

DEDICATION

This work is dedicated to the glory of the Almighty God, my grandmother Teresa Aina for her love and tender care, my wife Anthonia and my children Rachael and Pauline for being part of the success.

DECLARATION

I hereby declare that

(i) the report presented in this Thesis is the result of my original research;

(ii) this Thesis has not been submitted to any other institution for any award other than Ahmadu Bello University Zaria;

(iii) all inclusions from works other than this have been duly referenced and acknowledged.

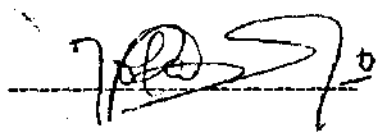

Adetola S. Oniku

17-08-99

Date

CERTIFICATION

This thesis entitled , a detailed study of the teleseismic P-wave travel time residuals at A.B.U seismic station Zaria, by Oniku, S. A., meets the regulation governing the award of Masters of Science Degree in Applied Geophysics of Ahmadu Bello University Zaria, and is approved for its contribution to knowledge and literary presentation.

Prof. S. B. Ojo — 20/08/99

Chairman, Supervisory Committee — Date

Prof. I. B. Osazuwa — 20/8/99

Member Supervisory Committee — Date

Prof. I. B. Osazuwa — 20/8/99

Head of Department of Physics — Date

Prof. S. B. Ojo — 08/06/00

Dean, Post gradute School — Date

ACKNOWLEDGEMENT

I wish to express my sincere gratitude to my able supervisor, Professor S.B. Ojo, who suggested this work and supplied all the materials needed. His ready-to-work attitude, high academic excellence and patience has encouraged me in the successful completion of this work.

I am also deeply indebted to Mr. Basil Eneh of the Institute of Seismology, University of Helsinki, Finland for sending some of the materials used in this work. Also to Professor I.B. Osazuwa, the Head of Department of Physics, for supplying part of the materials used, I say thank you for you are kind and good; just keep it up.

My gratitude and appreciation go to my colleagues, Dogara -Matoh, Kolawole Lawal, and Patrick Igbru for their being there in time of crises.

I express my sincere thanks to the authority of Federal University of Technology Yola, for approving the study fellowship.

Most of all, I thank God Almighty, author of all creature for sustaining me through thick and thin, giving me strength and hope when there were none left in me.

Finally, to my wife and my daughters, I say "thank you" for your understanding and encouragement.

ABSTRACT

The teleseismic P-wave travel time residuals at the Ahmadu Bello University (A.B.U.) Zaria seismic station were measured with respect to the Jeffery-Bullen (JB) tables. A total of two hundred and thirty (230) events at epicentral distances between 24° and 180° was selected from recordings covering the period January 1985 to December, 1992. The limited number of events used was due to the low operational gain (due to high cultural background noise) at the station which permitted only events whose magnitudes are large enough to be picked. This was further reduced to 108 events which have residuals less or equal to 5.

The data obtained were used to create the station history plots which display the travel-times on the distance-time curve, event locations on a world map centered at Zaria and the P-wave residuals for the station.

The station absolute residuals for all the selected events vary between -4.1 s to 5.0 s with an average value of 1.08 s ± 2.0 s. The azimuthal biases were then taken into consideration by sorting the residuals into 10° azimuth by 10° distance bins. A new station average residual was calculated to be 0.72 ± 1.81 s by summing over the average residual for that bin. These are then referred to as the residuals before and after sorting respectively. The large standard deviation of the average residuals suggests that the variation in the residuals cannot be accounted for by considering the data as belonging to one homogeneous set. The data set was therefore sub-divided into five regions on the basis of similar azimuths and propagation path to the station. The average residuals for each of the five regions are:

(i) Mediterranian +1.05±0.85s

(ii) Kazakhstan -0.90+0.40 s

(iii) Burma/lndia/China +2.33+1.18 s

(iv) South and Central America +1.40+1.00 s

(v) North Ascension Island +0.20+0.70 s

Relative travel time residuals of the station were calculated with reference to some group of stations located in the stable West-African Craton, Congo Craton and the seismically active East-African rift valley by considering some events distributed randomly in the five different regions. It was found that the trend of the relative residuals is an indication of lateral inhomogeneity of the crust and upper mantle between the various stations and Zaria station. It was also found that the relative residuals are highly dependent on the direction of approach of the P-waves.

An inversion of the travel time data was attempted using the tau-p method of inversion. However the observed data were found to be too few and sparse in any given azimuth to yield meaningful results.

-

CONTENTS

Title.....i

Dedication.....ii

Declaration.....iii

Certification.....iv

Acknowledgement.....v

Abstract vi

TableofContents.....viii

List of figures..... xi

List of Appendices.....xiii

CHAPTER ONE

1.1 General Background.....1

1.2 Aim of theStudy.....2

1.3 PreviousStudy.....3

1.4 Choice of Technique.....5

CHAPTER TWO

BRIEF GEOLOGY OF THE WEST-AFRICAN SUB-REGION

2.1 Introduction.....7

2.2 The West AfricanCraton..... ..9

2.3 The Pan-African Mobile Zone.....10

2.4 Lithospheric Structure of West Africa from seismological and Heat flow data

2.4.1 Seismological Data.....12

2.4.2 Heat Flow Data.....13

2.5 Brief Geology of the station Region.....14

CHAPTER THREE

THEORY, METHODOLOGY AND INSTRUMENTATION

3.1 Seismic Waves....16

3.2 Seismic Rays in a spherically stratified earth 17

3.2.1 The Ray Parameter p of a seismic wave 17

3.2.2 General Expression for T and Δ....21

3.3 Methodology....24

3.3.1 Travel time Residual 24

3.3.2 Extremal Inversion of Travel time data.... 26

3.4 Instrumentation....29

CHAPTER FOUR

DATA AQUISITION AND INTERPRETATION

4.1 Data Aquisition 35

4.1 Interpretation of Results....36

4.2.1 Station History 36

4.2.2 Azimuthal variation of Travel time Residuals....42

4.2.3 Relative Residuals....52

4.3 Velocity Inversion 56

CHAPTER FIVE

DISCUSSION AND CONCLUSION 61

REFERENCES 65

APPENDICES

Appendix I 70

Appendix II....76

Appendix III.... 82

List of Figures

		Page
Fig. 2,1	Map showing the three well formed African Cratons	8
Fig. 2.2	West African Craton's major outcrops and the Pan-African mobile zone	11
Fig. 3.1:	Teleseismic ray in a three layer earth	19
Fig. 3.2:	Adjacent teleseismic rays with geometrical construction used to derive equation 3.6	19
Fig. 3.3	Geometry used to obtain the integral expresion for	22
Fig. 3.4:	MEQ 800 Functional block diagram	30
Fig. 3.5:	Typical seismogram mark	32
Fig. 3.6	Maximum sensitivity characteristics	34
Fig. 4.1:	Relative positions of some selected seismic stations in West, Central and East Africa	37
Fig. 4.2:	Events location centred on Zaria	38
Fig. 4.3:	Travel time plot for all events observed	40
Fig. 4.4:	Travel time plot for sorted events	41
Fig. 4.5:	Frequency distribution of P - phases	44
Fig. 4.6:	Station residual plot centred on Zaria	46
Fig. 4.7:	Plot of average residual versus back azimuth	47

Fig. 4.8: Residual plot of AAE (Addis-Ababa) 49

Fig. 4.9: Residual plot of LWI (Lwiro) 50

Fig. 4.10: Residual plot of KIC (Kosan-Boka) 51

Fig. 4.11: Residual plot of NAI (Nairobi) 52

Fig. 4.12: Azimuthal distribution of events versus distance (deg) 57

Fig. 4.13: Plot of time - distance curve for continental region 58

Fig. 4.14: Plot of reduced travel time versus distance 60

List of Appendices

Page

Appendix I : List of all selected events 70

Appendix II : List of events with absolute residual < 5.0 s 76

Appendix III : List of events used in computing relative residuals 82

CHAPTER ONE

INTRODUCTION

1.1 General Background

Teleseismic P-wave travel time residuals find useful applications in the study of crustal and upper mantle structure especially with regards to the geodynamic processes taking place in these regions. The basic assumption of the method is that seismic wave velocities vary not only as a function of the dilatant behavior within the stressed medium, but also with changes in the state of the material caused by external processes such as heat, pressure and other similar factors. It is, therefore, of interest and practical importance to monitor tectonic regions for velocity changes. A distinct velocity difference is expected, for example, between stable shield regions and regions of recent tectonic activity. These variations manifest themselves in many ways, including:

1. regional deviations from standard velocity-depth functions.
2. lateral variation of crustal structure
3. lateral variation of the upper mantle low velocity layer
4. lateral inhomogeneities in the lower mantle.

One approach to the study of this effect is to use the large number of recorded teleseismic earthquakes as signal sources to monitor P-wave travel-time residuals in order to isolate velocity changes occurring in the vicinity of the receiver. This approach is useful, for example, in regions without local networks and of low seismicity, such as in Nigeria where velocity data on a local scale is not available.

However, travel-time residuals suffer a major difficulty in isolating that part of it associated with changes in crustal velocity near the receiver from travel-time variations produced by earth structure near earthquake source and along paths within the lower mantle. For this reason, the station residuals may be isolated by independent studies of the area around the station region(e.g. seismic refraction studies) or through the relative residuals. Relative travel-time residuals are computed relative to a reference station in a group, and ensures that the residuals are not limited by the uncertainty of the absolute value of the travel-time but by that of the slope of the travel-time standard (Agarwal et al.; 1976).

1.2 Aim of the Study

The present work is a detailed study of the teleseismic P-wave arrival times of events recorded at the Ahmadu Bello University (A.B.U.) seismic station, Zaria. The observed arrival-times are then used to determine the travel-time of the events with a view to establishing the absolute travel-time residuals of the seismic events. These are then used to study the geodynamic processes taking place along the propagation path and to establish the velocity structure beneath the propagation path. The study is made up of the following components:

1. Creation of a data base for all seismic events recorded at the station, so as to facilitate access to the station data.
2. Establishment of the station history of Zaria. This includes the plot of raw data of travel time versus epicentral distance,showing all the events on map of the world with Zaria as the center, and plotting the histogram of residual with the

frequency of occurrence.

3. To establish the relative travel time residual between Zaria and some nearby stations in West Africa, Central Africa and East Africa so that the effect due to travel time variations produced by the earth structure could be reduced to that of the earth structure along the propagation path.
4. To investigate the gross properties of the travel time residuals, taken into consideration the azimuthal dependence of the residuals.
5. To determine the velocity structure along the propagation path using an inversion technique based on tau method (Bessonova et al. 1974, 1976).

1.3 Previous Studies

In Nigeria, Earthquake studies have been at a low level prior to the 1984 earth tremors which occurred at Ijebu-ode, South-western Nigeria. Since then, the need to study earth structures in Nigeria to better predict possible future occurrence of earthquakes and other natural disasters has been a major concern. This formed the basis of the organization of a National seminar on earthquakes in Nigeria held at the A.B.U. Zaria in 1985 (Ajakaiye et al.,1989). The seminar focussed attention on the theme "The implications of earthquakes in Nigeria" with the following sub-themes:

i. Detection and prediction of earthquakes

ii. Historical perspective of earthquakes in West Africa

iii. Faults/Fractures in the Nigerian landmass

iv. Engineering design considerations for earthquake prone areas.

Other publications on earthquakes in Nigeria include that of Ajakaiye et al. (1987) on the July 28, 1984 Southwestern Nigeria earthquake and that of Ige (1984) on the December 21, 1975 tremor near Fagwalawar Garu in Dambata, Kano.

Prior to the present study, several authors have used travel time residuals to get information on crustal and upper mantle structures and also the geodynamic processes at work. Ojo (1994) studied the teleseismic P-wave travel time residuals at the A.B.U. Zaria station and concluded that there is significant consistency in travel times of earthquakes within each of the three regions investigated thus suggesting that the quality of the data obtained at the station is satisfactory. Also, the pattern of variation of the residuals yields some insight into the differences in structure of the upper mantle in the three regions studied.

P-wave travel time residuals have also been used to investigate tectonic activities and to delineate structures in many island arcs especially in the Aegean region (Agarwal et al., 1976; Gregersen, 1977; Panagiotopoulos et al., 1985). Panagiotopoulos et al (1985) studied the travel time residuals in South-eastern Europe and concluded that the crust in this region is continental. Engdahl et al (1977) used relative teleseismic P-wave travel-time residuals between Alaskan-Aleutian stations to examine the plate structure beneath Alaska.

1.4 Choice of Technique

The Ahmadu Bello University Seismic Station, Zaria was installed in 1983 with the primary aim of monitoring earthquakes or earth tremors in order to establish the level of seismicity in the country. Shortly after the installation, an earthquake of intensity IV occurred in Ijebu-Ode area in 1984 justifying the station. Another earthquake with body wave magnitude 4 occurred causing damages to houses in the Gembu area of Taraba State in January 1987. All other earthquakes recorded at the station were of regional and telesesmic distances.

The choice of technique used in the study is borne out of the fact that the travel times of seismic events are usually affected by effect from the source region, propagation path and the station region. Therefore, seismic waves travelling from source to a recording station could either travel faster or slower, that is have negative or positive residuals, respectively, depending on the propagation path (Ojo, 1994). Also, the use of relative travel time residuals is justified because of the non-uniqueness of the absolute travel time residual (Agarwal et al .; 1976). Accordingly, it was decided to use the relative time residuals of Zaria station with respect to some nearby stations in West, Central and East Africa. Zaria station was chosen as a reference station because of its central location compared to the stations in Cote D'Ivoire, Ghana, Cameroon, Central Africa Republic and Zaire and Kenya. The effect of this is to reduce the influence on the travel time residual to that due to station region only.

Finally, since the travel-time residuals provide only gross information about the station region, an attempt was made to invert the travel time data using the tau-p method of inversion (Bessonova et al.; 1974, 1976). This method is simple because it neither involves estimation of p, the ray parameter, by numerical differentiation of travel times nor involves interpolation of the travel-time curve between actual observations. The function is estimated directly from the observed travel times and distances (T_i, X_i).

CHAPTER TWO

BRIEF GEOLOGY OF THE WEST AFRICAN SUB-REGION

2.1 Introduction

The Geology of Africa is dominated by the Kalahari, Congo/Zaire and West-African Cratons (Fig. 2.1). These are composed of Late Archean and early-middle Proterozoic crystalline basement rocks which are non-conformably overlain by middle to late Proterozoic - earliest Paleozoic shelf sedimentary sequence and successions within younger Paleozoic basins (Clifford, 1970). Kennedy (1964) noted the dominance of 650-450 m.y. K-Ar ages in the upper Precambrian terrains but did not recognise indications of the classic orogenesis in the non-Archean terrains, except in the Danara-Katanga belt, and hence used the term "*Pan-African thermo-tectonic event*" to identify major episode in the African geological evolution.

The major geological features in West-Africa are mainly the West-African Precambrian Craton with its sedimentary cover and the surrounding mobile belts, largely of Upper Proterozoic age but locally affected by Paleozoic overprinting. Black and Caby (1979) showed that Late Precambrian orogeny referred to as Dahomeyide Orogeny in the south eastern part of the Craton took place at Hogger, Nigeria and Dahomey, followed in the early Palaeozoic by several post-tectonic granitic intrusions.

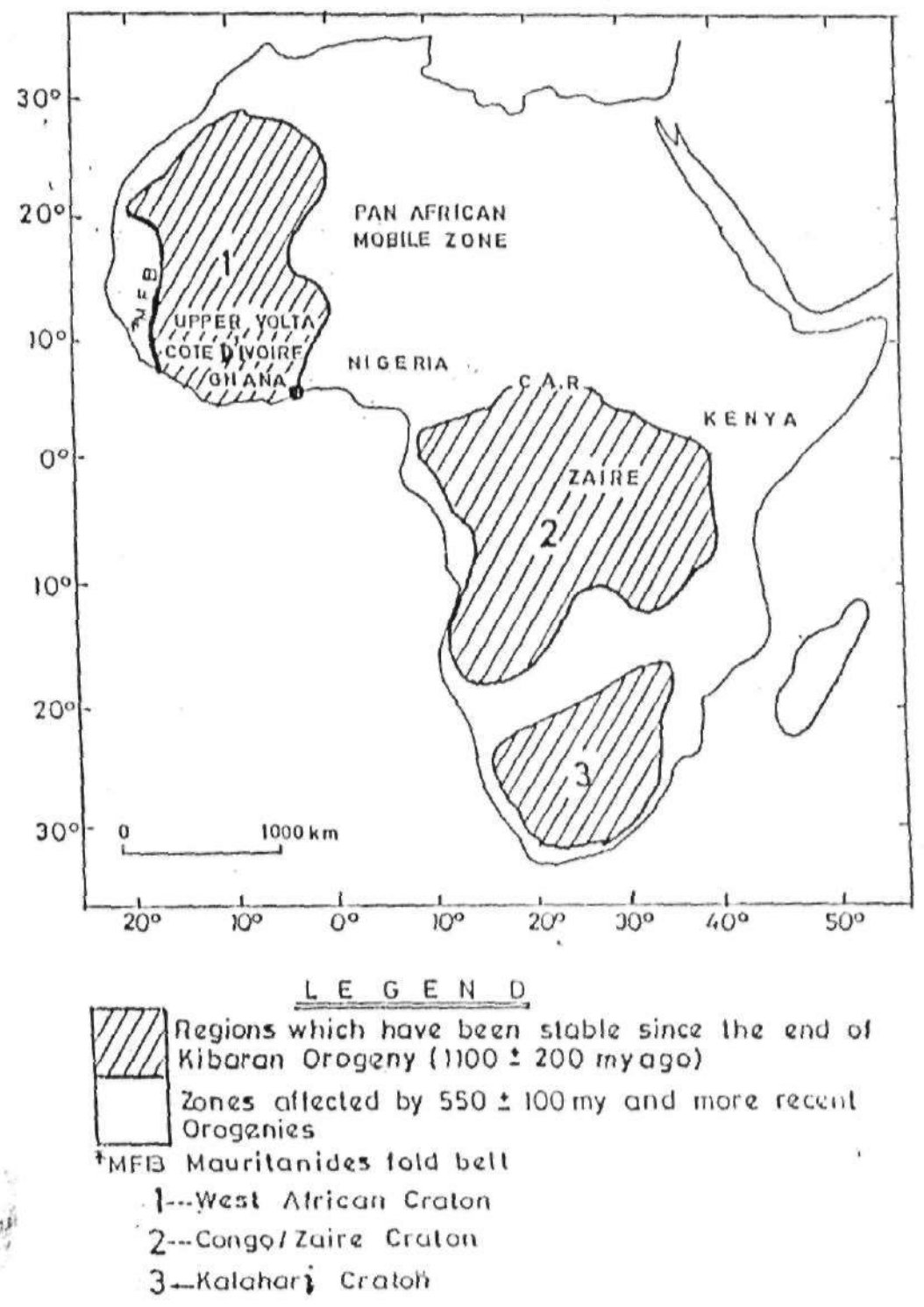

FIG. 2.1: Map showing the three well formed African cratons

2.2 The West - African Craton

The West-African Craton is a very extensive portion of Precambrian crust extending approximately 4.5 million km^2 (Rocci et al.; 1991), located approximately within Longitudes 0° and 15° 5'W and Latitudes 25° 15'N and 4°45'N . It is stable since 1700 m.y. ago, and bounded on all sides by more recent mobile belts mainly of Pan-African age, such as the Mauritanide fold belt on the Western edge and the Pan-African mobile belt on the eastern edge (Fig. 2.1).

More than half of the craton is covered by sediments of upper Proterozoic to Late Paleozoic sediments of the Taudeni basin. The West African craton crops out in two main Uplifts; the Leo Shield in the South and the Reguibat shield in the North (Rocci et al.; 1991). It is formed essentially of two Precambrian Cratonic basement (Bessoles, 1977). These are the Late Archean rocks dated about 2,750 - 2,600 m.y. and the early Proterozoic or Birrimian rocks mainly affected by the Eburnean Orogeny (2000-1800 m.y.).

The Late Archean rocks are exposed in the South-western part of the Reguibat Shield (Barre're, 1976) and in the western portion of the Leo Shield, while the early Proteroic or Birrimian rocks are the main parts of the cratonic basement in the Leo Shield. They also make up the northeastern part of the Reguibat Shield. In the Leo Shield, especially in Burkina Faso (Upper Volta) and Cote D'Ivoire, geochronological data suggest a Burkinian Cycle (2400-2100 m.y.) distinct from the

Eburnean Orogeny (Caen - Vachetter, 1988). Granites were emplaced between 2000 and 1700 m.y. (Vachette et al.; 1975). These intrusions mark the end of the crustal evolution of the West African Craton and it has been stable since then.

2.3 The Pan - African Mobile Zone

This zone was first mentioned by Kennedy (1964) as a main tectonothermal episode which affected the borders of the previously Cratonized West African craton at 550±100 m.y. They comprise the Haggar massif (or Touareg Shield) to the North, and to the South, Dahomean - Nigeria horst (Fig. 2.2). It is located to the East of the West-African craton. The Pharusian - Dahomean Orogens which extends through Hoggar in Algeria (Bertrand and Caby, 1977), the Iforas and Gourma regions in Mali (Reichelt, 1972; Caby, 1987) and the Dahomean chain in Benin and Togo (Affaton, 1975; Trompette, 1979) are interpreted as the result of an oceanic closure and collision around 600 m.y. (Black and Caby , 1979) between the West African passive margin and an eastern continent including the Hoggar Shield and the Benin and Nigeria Shields. The Pan-African suture which marks the boundaries between thermally activated areas and cratons and also the site of ocean closed through paratectonic orogeny can be traced from Morocco to Togo (Leblanc 1976; Black and Caby, 1979).

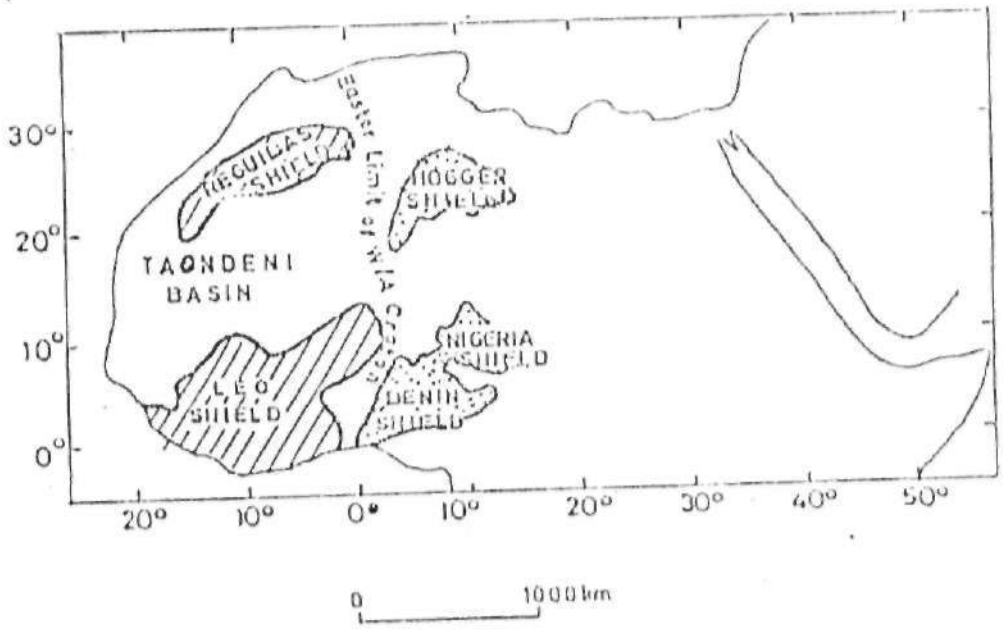

FIG. 2.2: West African craton's major outcrops and the Pan African mobile zone

2.4 Lithospheric Structure of West Africa from Seismological and Heat Flow Data

2.4.1 Seismological Data

P-wave studies of the West African craton margin in Senegal (Briden et al., 1981; Dorbath et al., 1983) revealed that a major seismic discontinuity, extending down to 150 - 200 km, separates the cratonic structural block which is characterized by highest velocities (Roussel and Lesqoer, 1991) from the Western Mobile zone.

The study of surface wave velocities along paths crossing the African continent (Dorbath and Montaguer, 1983) provides models for vertical distribution of lithospheric velocities and allows the generalization of the Local P-wave results to the whole continent. The model shows that the cratonic areas are characterized by higher shear-wave velocities than mobile zones. The model, however, does not account for lateral inhomogeneities within the lithosphere because only a few distinct paths are considered and also because an a priori crude regionalization in craton and mobile zones is used for data inversion (Roussel and Lesqoer, 1991).

A recent interpretation of long period records of surface waves (Hadiouche and Jobert, 1988) without any a priori geological constraints improves the lateral resolution and provides a more accurate three dimensional image of the lithospheric structure beneath Africa. Hence, Hadiouche and Jobert (1988) explain that the West African craton is characterized by a fast lithosphere to a depth of 240 km, whereas

the Pan-African eastern mobile belt is characterized by a slow lithospheric zone 150 km thick which trends NW - SE and extends from Sahara to Red Sea.

2.4.2 Heat Flow Data

Heat flow density values in West - Africa can be discussed in the context of two major tectonic unit; the West African craton and the mobile belt. The Eburnean Leo Shield which covers the entire Cote D'Ivoire and Western and Northern Ghana (Fig. 2.2) is characterized by an average heat flow (30 ± 10 m Wm^{-2}) lower than on the Pan - African basement of the Hogger (Touareg) and Benin - Nigeria Shields (51 ± 8 m Wm^{-2}) (Roussel and Lesqoer, 1991). These values are comparable with those observed within other shields and reveal a generally decreasing heat flow with tectonic age, which is the general world wide rule (Vitorello and Pollack, 1987).

The difference in average heat flow density between cratonic domain and surrounding mobile belts seems to be significant and may be interpreted as being due to greater crustal heat production within mobile belts than in cratons, or alternatively due to differences in lithosphere deep structure (Ballard and Pollack, 1987).

The present lack of heat production data and of information on the deep crust structure does not allow the interpretation of heat flow density in relation to crustal inhomogeneities (Roussel and Lesqoer, 1991). However, magnetotelluric

results (Ritz and Robinean, 1976) reveals that the southern part of the West African craton is characterised by a high resistivity.Seismic results (Dorbath and Dorbath, 1984; Hadiouche and Jobert, 1988) and geotherm heat calculation (Roussel and Lesqoer, 1991), lead to the proposal that the southern part of the West African craton is characterised by a high velocity and low temperature.

2.5 Brief Geology of the Station Region

The Ahmadu Bello University Seismic Station, Zaria, Nigeria has station coordinates given by a latitude of 11.150°N and longitude 7.654°E. The region is belongs to the Precambrian Basement Complex which is believed to have been affected by four Orogenic cycles (Odeyemi, 1978). These are the Liberian event (2800 - 2500 m.y.), the Eburnian episode (2150 m.y.), the Kibaran Orogeny (1300 - 900 m.y.) and the Pan African Orogeny (650 m.y.). Based on the work of McCurry (1970) and Webb (1972), the principal rock units are classified as follows:

i) a crystalline basement complex composed of gneisses, considered to have been metamorphosed more than 2000 m.y. ago;

ii) older granites that intruded the gneisses crystalline complex from 647 to 618 m.y. ago. They have an approximately conformable relationship with the crystalline host rocks (McCurry, 1970).

Gneisses constitute the ancient crystalline basement, which probably underlies the entire area and accommodates the belt of metasediments. McCurry

(1970) postulated that the gneisses were sedimentary in origin. Adeniyi et al; (1992) in trying to investigate the structure of the older Granite suite and to infer its origin and mode of emplacement in relation to the surrounding metasediments and gnisses reveals that Zaria area is characterized by the granitic intrusives which he refers to as multiple Batholiths. The Zaria Batholith is sub-elliptical and oriented N-S. The strike length of the Batholith is approximately 32 km and its largest surface width is 13 km. The rock units listed above are compositionally similar in that they contain quartz, microcline, plagioclase and biotite as essential minerals with accessory apatite and zircon. Porphyroblastic biotite granite is the most common and most distintive of the granites. They are richly potassic with large microcline megacrysts. Discordant contacts show that most of the granites are intrusive, and flow features such as swirling foliation, rotated xenoliths and boundinage aplite veins and mafic pods are suggestive of movement in a semi-plastic condition (McCurry, 1970).

CHAPTER THREE

THEORY, METHODOLOGY AND INSTRUMENTATION.

3.1 Seismic Waves

The seismic or elastic waves, which are initiated through the sudden release of stress in an earthquake source region or by an explosion, propagate through the whole of the earth's interior or along its surface layers. The waves are recorded by remote seismic stations provided the energy released is large enough. Seismic waves are of two main types (Bath, 1979):

1. Body waves, which propagate through the interior of the earth. These consist of two types:
   (a) Longitudinal waves or P-waves
   (b) Transverse waves or S (or shear) waves.
2. Surface waves or guided waves, which propagate along the surface. These consist of the following types:
   (a) Love(L) and Rayleigh (R) waves which follow the free surface of the earth.
   (b) Stoneley waves, which are related to Rayleigh waves, but follow a discontinuity surface in the earth's interior.
   (c) Channel waves, which propagate along some layer of lower velocity in the earth's interior.

Body waves are considered as free waves, that is, they have freedom to propagate in practically every direction through the earth's interior while surface waves are bounded to some surface or layer during their propagation.

This study deals with the P-phase (or P-wave) i.e. part of body waves. For that reason, only the theory as related to body waves in general and P-waves in particular will be treated in this chapter. In the treatment, it would be assumed that:

1) The earth is a sphere and all layers have the same curvature;
2) The properties of the earth vary with depth and, in general, the wave velocities increase with depth.

3.2 Seismic Ray in a Spherically Stratified Earth.

3.2.1 The Ray Parameter p of a Seismic Wave.

As body waves propagate through the earth's interior, they follow the same laws which hold for any other wave propagation, for instance in optics. The most important relation is Snell's law of refraction, which is generally written as:

$$n \sin i = \text{constant} \qquad \text{.....(3.1)}$$

along a given wave path, where

n = refractive index of the medium,

I = angle of incidence of the wave.

In term of the ray velocity,v, the equation (3.1) is re-written as

$$\frac{\sin i}{v} = \text{const.} \qquad \text{.....(3.2)}$$

To apply this to our earth model, we assume that the earth model is composed of an infinitely large number of thin concentric homogeneous shells (Bullen, 1985) across which there is a discrete velocity change. Consider portion PP_1P_2 (Fig. 3.1) of a seismic ray, where P,P_1,P_2 are points on three consecutive boundaries between these shells. Let v_1 and v_2 be the ray speed along PP_1 and P_1P_2 respectively; and let the angles be as in Fig.3.1. By applying ray geometry, we have;

$$\frac{Sin\ \theta_1}{v_1} = \frac{Sin\ \theta_2}{v_2} \qquad \text{.....(3.3a)}$$

$$\frac{OP_2\ Sin\ \theta_1}{v_2} = \frac{OP_2\ Sin\ \alpha}{v_3} \qquad \text{.....(3.3b)}$$

But,

$$OP_1 Sin\ \alpha = OP_2\ Sin\ \theta_2 \qquad \text{.....(3.4)}$$

where P,P_1 and P_2 are points on three consecutive boundaries between these shells. O is the centre of the earth. The equation (3.4) represents the expression for the perpendicular from O to P_1P_2.

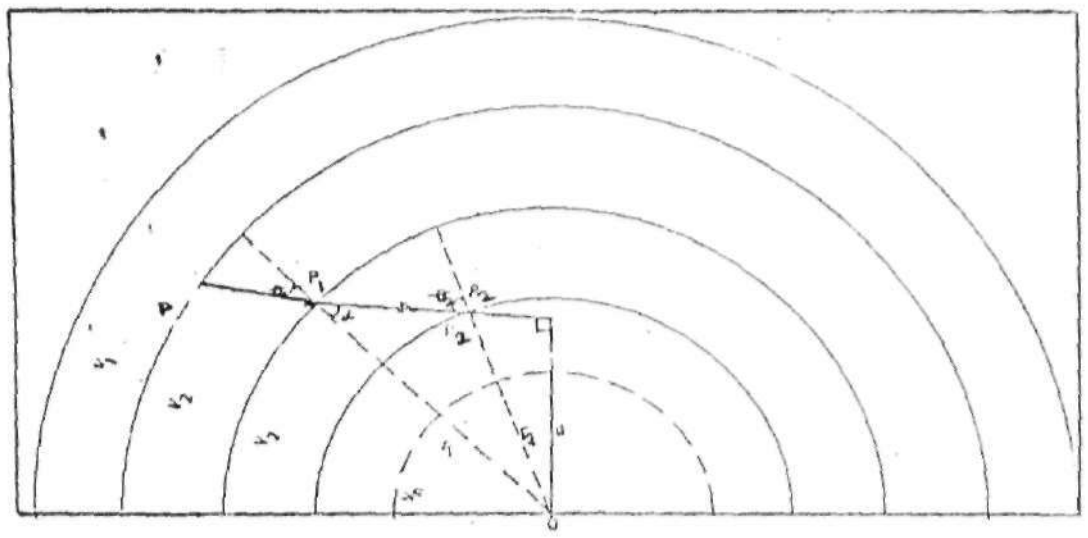

FIG. 3.1: Teleseismic ray in a three layer Earth.

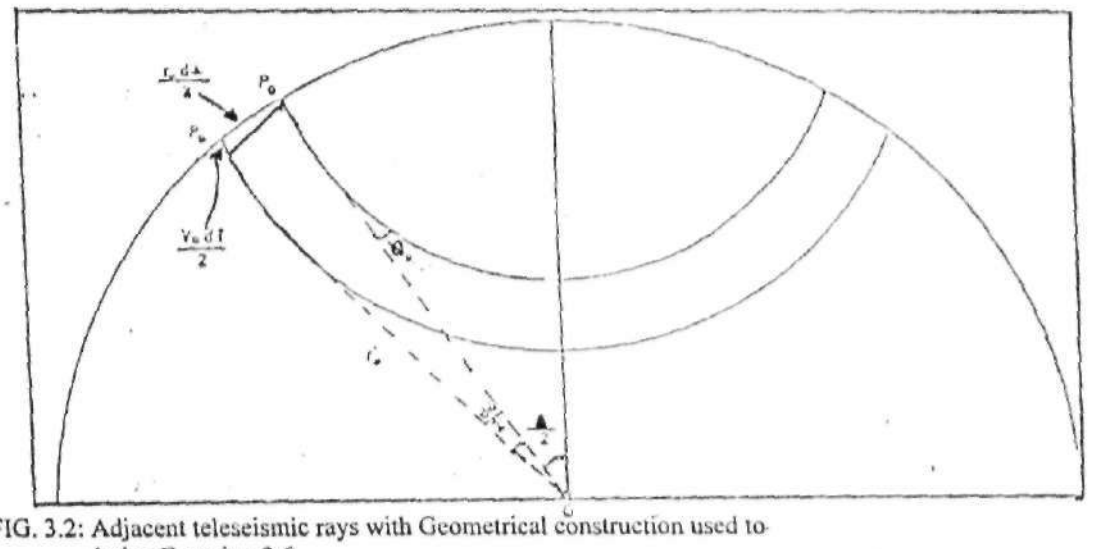

FIG. 3.2: Adjacent teleseismic rays with Geometrical construction used to derive Equation 3.6

Therefore, substituting equation (3.4) in (3.3b) we have,

$$\frac{0P_1 \sin \theta_1}{v_2} = \frac{0P_1 \sin \theta_2}{v_3}$$

Since v = v(r), therefore,

$$\frac{r \sin \theta}{v} = \text{Constant} = p \qquad \text{.....(3.5)}$$

where p is referred to as the ray parameter and is a constant for a given ray.

The ray parameter bears a remarkable relationship to the travel-time curve. The relationship is expressed in (Fig. 3.2). Ray P_o which has an inclination θ_o has a travel time T over an arc distance Δ. An adjacent ray P would also have a travel time T + dT over an arc distance $\Delta + d\Delta$.

From ray geometry,

$$\sin \theta_o = \frac{v_o \, dT/2}{r_o \, d\Delta/2}$$

where r_o = outer radius

Therefore, by transposition

$$\frac{r_o \sin \theta_o}{v_o} = \frac{dT}{d\Delta} = p \qquad \text{.....(3.6)}$$

This implies that the parameter p is the slope of the time-distance curve at a

distance Δ from the source, and dT/dΔ which has the dimensions of inverse velocity is called the slowness.

3.2.2 General Expression for T and Δ.

Considering figure 3.3, let the coordinates of a point P along the ray be r and θ.

From ray geometry,

$$\sin i_0 = r \frac{d\theta}{ds}$$

But, the ray parameter, p is given by :

$$p = \frac{r \sin i}{v} = \frac{r^2 \, d\theta}{v \, ds} \qquad \text{.....(3.7)}$$

By re-arranging equation 3.7

$$ds = \frac{r^2 \, d\theta}{p \, v} \qquad \text{.....(3.8)}$$

Also,

$$d\theta = pv \frac{ds}{r^2} \qquad \text{.....(3.9)}$$

The arc distance along the ray is given as

$$(ds)^2 = r^2(d\theta)^2 + (dr)^2 \qquad \text{.....(3.10)}$$

Substituting (3.8) in (3.10), we have

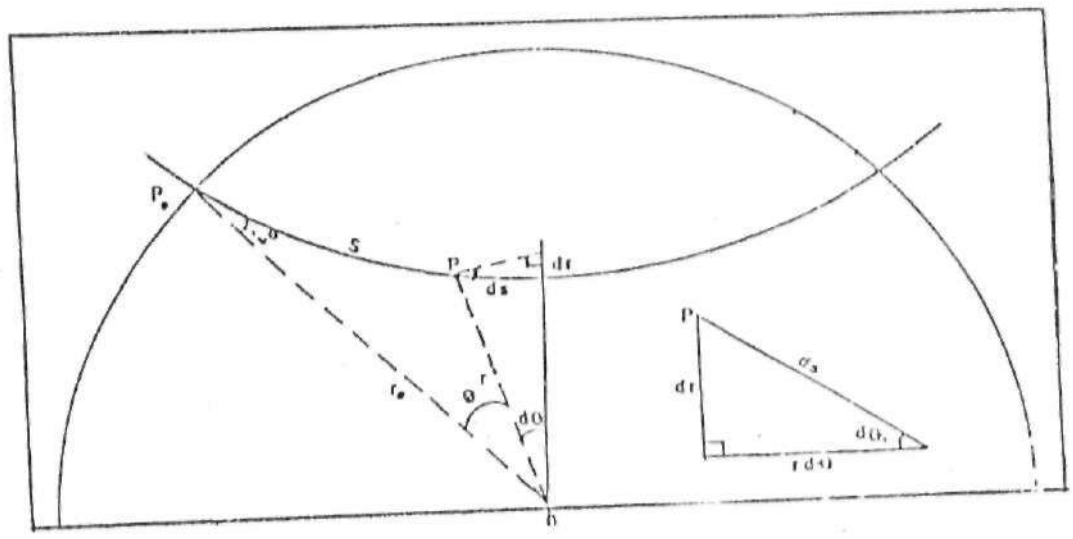

FIG. 3.3: Geometry used to obtain the integral expression for Δ

$$\frac{r^4\,(d\theta)^2}{p^2\,v^2} = (dr)^2 + r^2(d\theta)^2 \qquad \text{.....(3.11)}$$

Solving for dΘ in (3.11), we have

$$\frac{dr}{r\sqrt{\frac{r^2}{v^2p^2} - 1}} \qquad \text{.....(3.12)}$$

Let p = r/v .....(3.13)

Hence equation (3.12) becomes

$$d\theta = \frac{p\,dr}{r\sqrt{(\rho^2 - p^2)}} \qquad \text{.....(3.13b)}$$

At the deepest point P (i.e mid point) of the ray

Sin i = 1, therefore,

$$p = P$$

If we integrate along the ray between the deepest point

r_p of the ray and the outer radius r_o, we have

$$\frac{\Delta}{2} = p\int_{r_o}^{r_p} \frac{dr}{r\sqrt{(\rho^2 - p^2)}} \qquad \text{.....(3.14)}$$

This gives the integral equation for the epicentral distance Δ.

Also, substituting (3.9) in (3.10), we have

$$(ds)^2 = \frac{p^2v^2}{r^2}(ds)^2 + (dr)^2 \qquad \text{.....(3.15)}$$

Simplifying this equation, we have

$$ds = \frac{dr}{\sqrt{1-\left(\frac{p^2v^2}{r^2}\right)}} \qquad \text{.....(3.16)}$$

Substituting equation (3.13)

$$ds = \rho\frac{dr}{\sqrt{\rho^2-p^2}} \qquad \text{.....(3.17)}$$

Therefore, the total travel time of the ray is given as

$$T = 2\int_{r_o}^{r_p}\frac{ds}{v} \qquad \text{.....(3.18)}$$

3.3 Methodology

3.3.1 Travel-Time Residual

A travel-time residual is defined as the difference between the observed travel-time of the seismic wave and the theoretical as obtained from the J-B tables. In the computation of travel times, the following conditions must be satisfied:

1) Focal parameters of an earthquake, i.e. geographical coordinates, focal depth, and the origin time t_o, must be accurately known.

2. Accurate measurement of the arrival time, t_a, of the seismic phase of interest at the observing station must be made.

3. Geographical coordinates of the station must also be known in order to determine the epicentral distance of the earthquake from the station.

4. There must be the existence of a standard travel time table which describes the travel time, T, as a function of epicentral distance, Δ and focal depth, h. This gives the theoretical travel time $T_c = T(\Delta,h)$ for a standard earth model. The observed travel time is given as

$$T_o = t_a - t_o$$

while the absolute travel time residual is defined as

$$R = T_o - T_c \qquad \text{.....(3.19)}$$

For this study, the focal parameters were obtained from the monthly listings of the Preliminary Determination of Epicentres (PDE) published by the United States Geological Survey (USGS) National Earthquake Information Centre. The seismic phase used was P-phase and the Jeffreys-Bullen (J-B) travel time tables (Jeffreys and Bullen, 1970) were used to obtain the theoretical travel times. Usually, travel time residuals are made up of contributions from the source region, propagation path and the station region. Therefore, a common problem in the analysis of travel times is how to distinguish between these components and also errors in the

standard travel time table. This problem is greatest at small epicentral distance where the angle of incidence is large, and travel paths in the source and station regions are insignificant (Ojo, 1994). Therefore, to correct for this, this study employs relative travel time residuals which are computed relative to a reference station in a group. The expression is given by the equation below

$$T_{ij} = r_i - r_j \qquad \text{.....(3.20)}$$

where r_j is the reference station residual, and r_i is the residual reported from other stations. Equation (3.20) ensures that the residuals are not limited by the uncertainty of the absolute value of the travel time but only by that of the slope of the travel-time standard (Agarwal et al.; 1976). Source residuals may be indicated by comparison of the source area with its surroundings (Gregersen, 1977).

3.3.2 Extremal Inversion of Travel-Time Data

The travel times of body waves are given at a discrete set of points (X,T), X being the epicentral distance and T the travel time. The aim is then to obtain extremal bounds on the possible velocity-depth (V,Z) plane (V being the velocity and Z the depth) which fit the travel-time data.

These bounds themselves do not represent suitable velocity profiles which lie between the bounds (Kennett and Orcutt, 1976). The approach, however, recognizes the often stated fact that since only a finite data set is usually available, with observational errors, an infinite number of possible solutions to the inverse problem exist (Backus and Gilbert, 1968).

The results of this approach to travel time inversion is modestly represented in the literature. McMechan and Wiggins (1972) introduced a method for the determination of the envelope of possible velocity models, by constructing in the ray parameter-distance (p-Δ) plane, an envelope around the data. The envelope was defined by the scatter of the data points, the uncertainties in the measurements, and various assumptions regarding the behaviour of the curve. Bessonova et al. (1974, 1976) described a method for deriving extremal bounds on possible velocity models from estimates of bounds on the function tau(p) defined by;

$$\tau(p) = T(p) - pX(p) \qquad \text{.....(3.20)}$$

where p is the ray parameter, T is the travel time, and X is the epicentral distance.

Kennett (1976) compared the method of Bessonova et al. (1976) and the linearized inverse technique of Johnson and Gilbert (1972), which also used the function tau-p in which iterative improvement is made to a trial model until it is in agreement with the data. The major advantages of the tau method is that it

determines a set of minimum and maximum depths at which some computed velocities would occur for layers derived from a set of discrete slowness values, and minimum and maximum tau corresponding to each value of the slowness.

Another advantage is that tau is single - valued with respect to p, decreases monotonically with increasing p and it is continuous except at values of p corresponding to the tops of any low-velocity zone at which points it has a negative jump. The choice of tau(p) method in this study is dictated by the quality of data which is somehow limited by the relatively few data points available for the station, hence interpolation of the travel time data and differentiation to obtain p would not be very suitable. Tau bounds were therefore determined by using the technique of Bessonova et al. (1974) from the knowledge that the function:

$$\tau(X,p_o) = T(X) - p_oX \qquad \text{.....(3.21)}$$

has a single stationary point which is a maximum for the generally direct, and a minimum for the retrograde branch of the travel-time curve. The extreme value of the function is tau(p) for the ray parameter p_o.

The procedure was then to determine tau for the maxima or minima of reduced time (T - pX) versus distance plots for trial values of p. From equation (3.20), one finds that for an error in travel time δT and distance δX for a particular ray parameter p, the error in $\tau(p)$ will be approximately,

$$\delta\tau = \delta T - p_o \delta X \qquad \text{.....(3.22)}$$

This result is based on the fact that, for part of the travel-time curve with ray parameter p_o, an error δX in the epicentral distance leads to an error $-p_o\delta X$ in travel time. Based on Bessonova et al. (1974), it would be assumed that the errors in δX and δT are normally distributed and independent. The tau bounds were then constructed with the estimated standard error in T.

3.4 Instrumentation

The MEQ - 800 portable seismograph is the instrument used for event detection recording at the Zaria station. It is a self-contained, portable, wide range seismic recording system, and is primarily designed for site locations of very low (micro-earthquake) to moderately high levels of activity. It can also be used to monitor and record strong disturbances the through use of an optional external attenuator. The functional block diagram of theinstrument is shown in Fig. 3.4. The MEQ - 800 system is composed of the following interconnected assemblies:

i) A battery pack power supply unit,

ii) An amplifier and main control panel,

iii) A crystal clock, and

iv) A drum recorder.

The amplifier has a gain control panel with 60 dB to 120 dB values in 6 dB

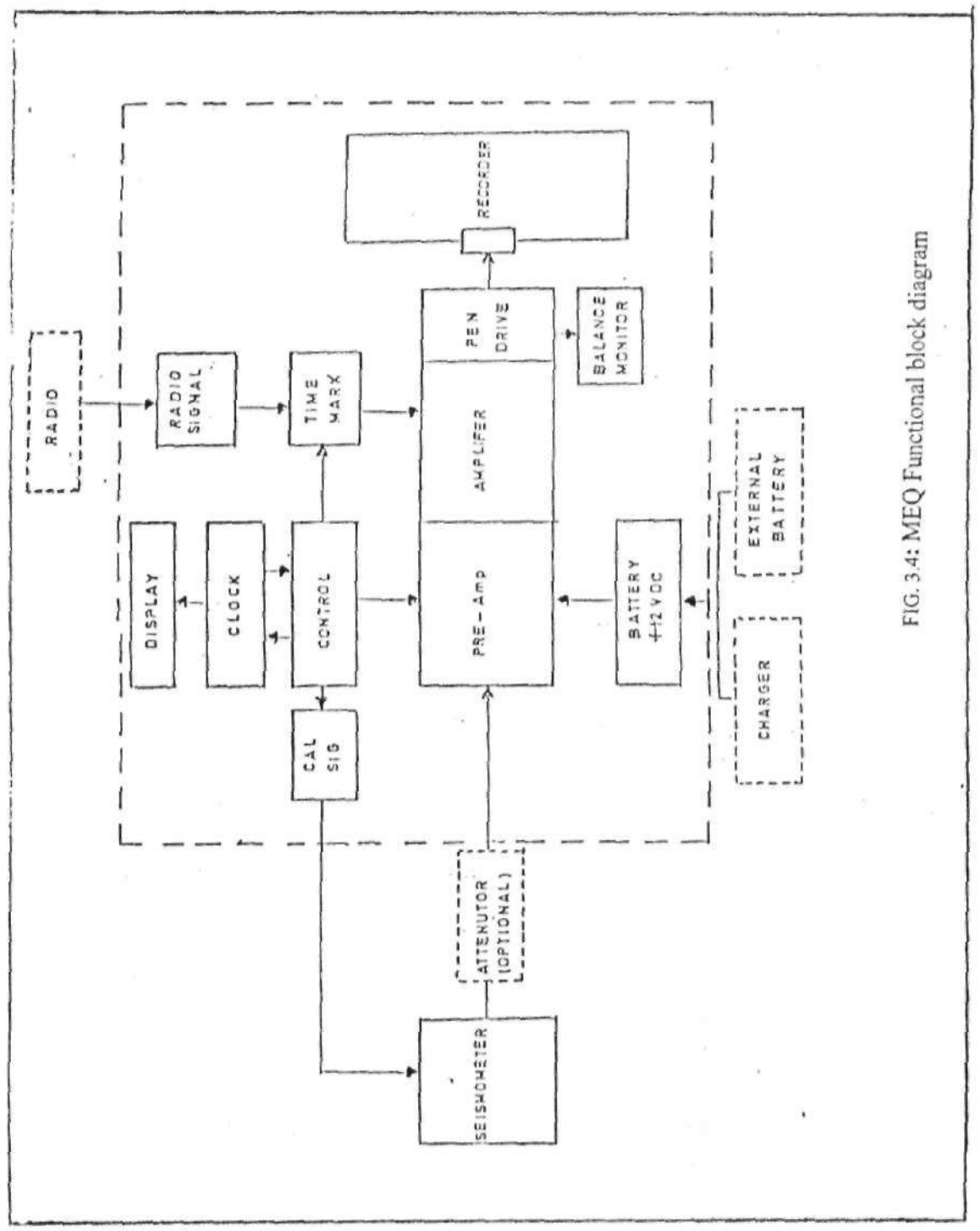

FIG. 3.4: MEQ Functional block diagram

increments (MEQ-800 Instrument manual). The gain stability is ±1%. The unfiltered frequency response is 3 dB points at 3 Hz and 70 Hz. The signal processing by the instrument is done by coupling the seismometer signals through the seismometer connector to the pre-amplifier via band pass and gain control networks. The amplifier having a low filter switch selects filters to set band pass lower edge limits at 3 Hz (low filter to out), 5 Hz or 10 Hz. Band pass upper edge limits are controlled by high filter switch at 5 Hz, 10 Hz or 70 Hz (Hi - filter to out).

Following conditioning in the filter and gain control networks, the signal is then applied to the pen deflection amplifier. Maximum pen deflection ranges of approximately 5 mm, 10 mm or 25 mm are determined by the amplitude limiting circuits and deflection switch. Accurate amplifier balance provides a reliable zero baseline reference for recording and aids in conserving battery power. The crystal controlled digital chronometer supplies a precise, highly stable (±4.32 ms/day throughout the 0°C to 50°C temperature range) time base for MEQ-800 record time references. "Time marks" are programmable in interval of seconds, minutes and hours (H m s) or minutes and hours (H m) only. A time mark of 10 seconds occurs at 12 Hrs and 24 Hrs (see Fig. 3.5). The drum recorder facilitates the MEQ - 800 record keeping. An electromechanically driven drum serves as the platform for the 343 x 600 mm seismogram (Ink recording type).

A Mark Products seismometer model L - 4C was used for all the measurements. It is a vertical component seismometer with 1 second period, 64

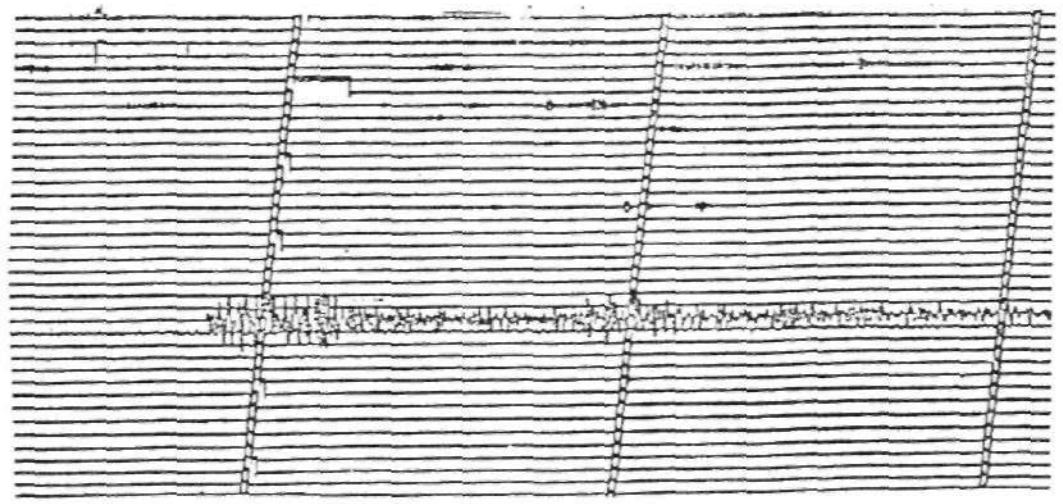

FIG:3.5 : Typical seismogram mark showing traces of P-wave arrival and time marks.

Ω damping, 5.5 k Coil. Depending on the relationship between the natural frequency of the external vibration, a seismometer functions as a measurer of displacement, velocity or acceleration of a seismic wave. The characteristic response curve of the seismometer is shown on Figure (3.6).

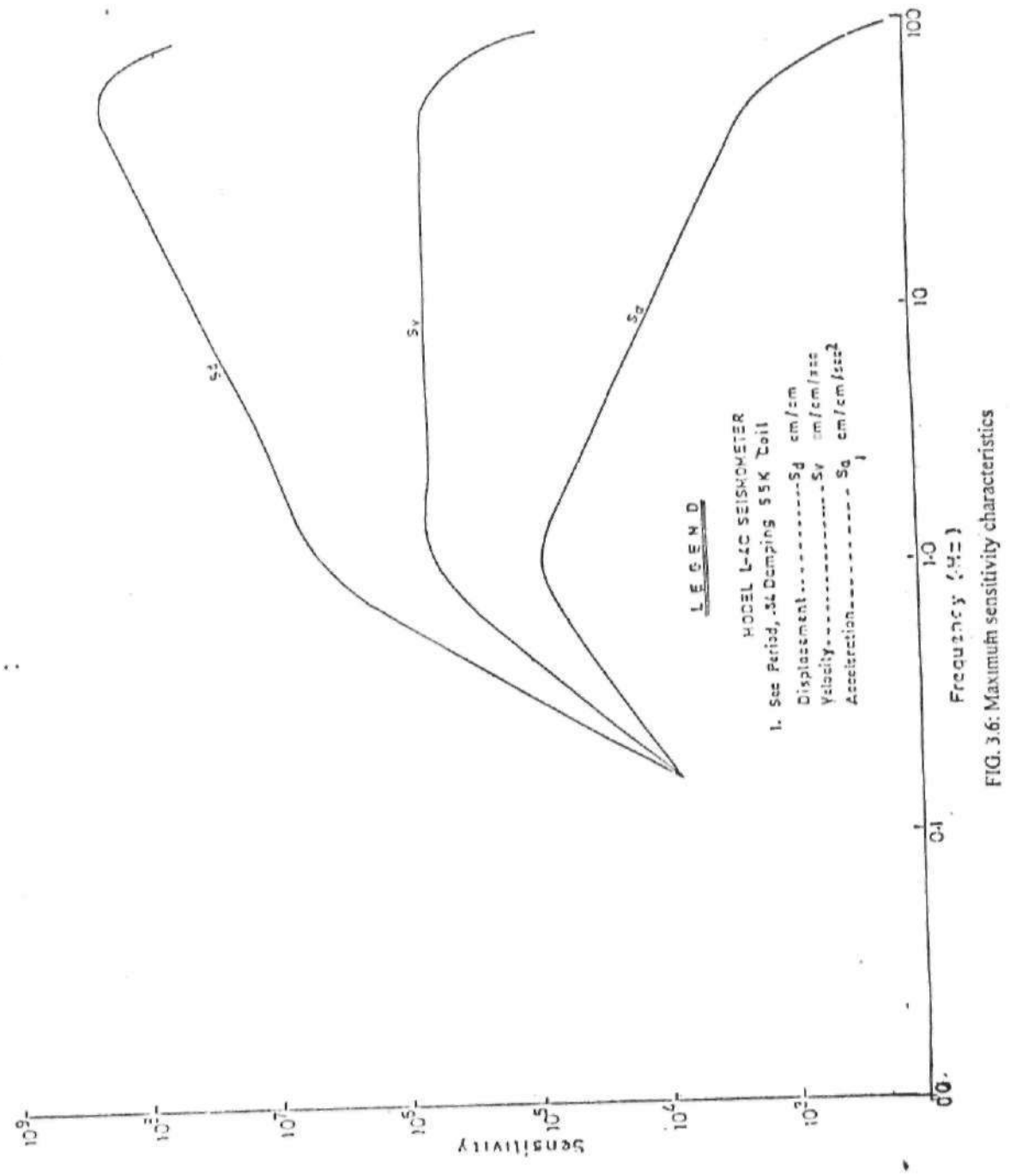

FIG. 3.6: Maximum sensitivity characteristics

CHAPTER FOUR

DATA AQUISITION AND INTERPRETATION.

4.1 Data Aquisition

The Ahmadu Bello University Seismic Station Zaria provided the data base used for this study. The arrival times of seismic events were picked off from seismograms recorded on daily basis since 1984 when the instrument was installed. However, because of the non-stability of the station in the first year of operation (Ojo, 1994), the data for 1984 were not considered reliable and only events from 1985 to 1992 were considered in this study. A total of two hundred and thirty (230) events were used.

A Computer program which was supplied by Prof. S.B. Ojo of Ahmadu Bello University, Zaria, computes the epicentral distance and the back azimuth of the events with respect to the station. From the distances computed and the listed focal depths of the events in the PDE monthly listings, theoretical travel time T_c were determined from the Jefferys - Bullen (1970) seismological tables. The first arrival times corresponding to P-waves were picked from the seismograms, and together with the origin times of the events given by the Preliminary Determination of Epicenters (PDE) monthly listings, observed travel times too were determined. The absolute travel time residual is then given by equation (3.19).

The absolute travel time residuals of some events for stations in Senegal, Cote D'Ivoire, Ghana, Central African Republic, Cameroon, Zaire and Kenya (Fig. 4.1) which were to be used to compute the relative travel time residuals were also obtained from the International Seismological Centre (ISC) Bulletins. About thirty (30) events which were recorded by almost all the stations were considered for this aspect of the study. The events have their sources azimuthally distributed randomly in five different regions, viz; Mediterranian, Kazakstan, Burma/India/China, North Ascension and South and Central America.

4.2 INTERPRETATION OF RESULTS

4.2.1 Station History

The data base for this study consisted of the two hundred and thirty (230) events carefully selected from the recorded events. Only events with a clear P-wave onset were selected. The events together with their source regions, focal depths and magnitudes are listed in Appendix I. The locations of the events are plotted in Figure 4.2 in equidistant azimuthal projection centred on Zaria. The plot is limited to events in the distance range up to 90 degree. Each concentric ring represents

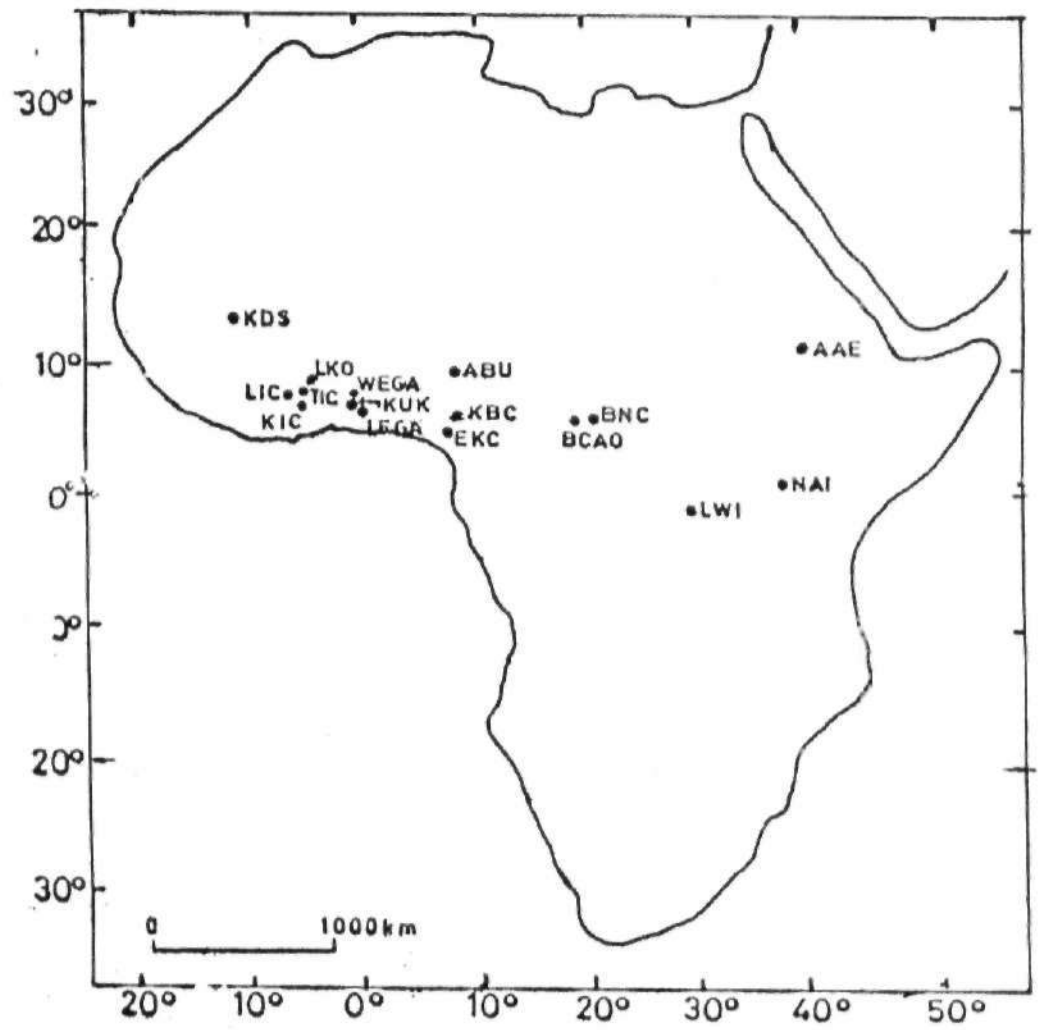

FIG. 4.1: Relative position of some selected seismic stations in West, Central and East Africa

POLE ABU

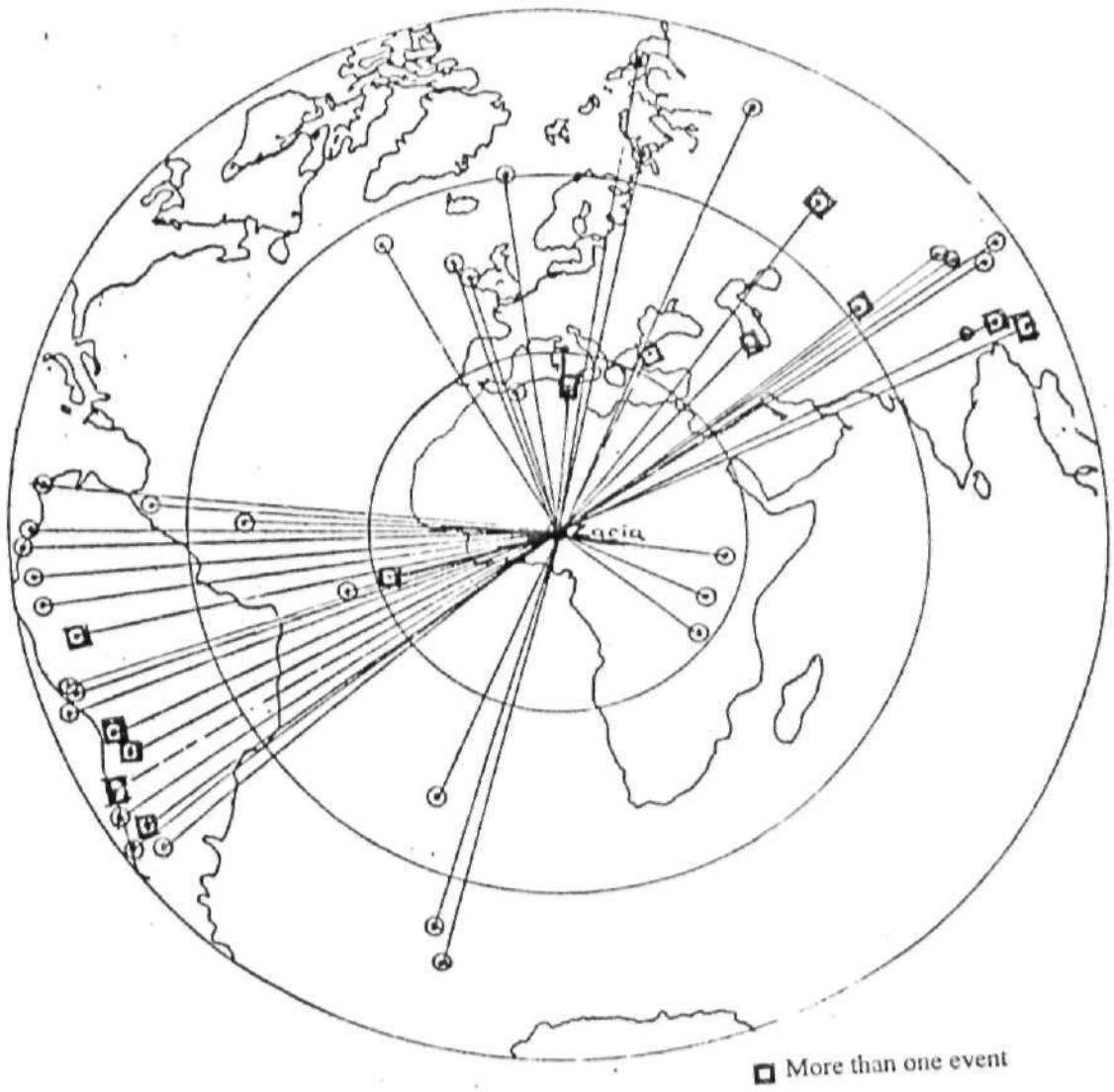

FIG. 4.2: Events Location Centred on Zaria.

an increament of 30 degree in epicentral distance. It is obvious from this plot that the data set is unevenly distributed in all quadrants. Dominant are events in the Mediterranian, East Kazakhstan, India/Burma/China, South and Central America and North Ascension Islands. A few events were reported from North Atlantic and other regions.

The plot of arrival times versus the epicentral distance in degrees of all events associated with Appendix I is shown in Figure 4.3. From this plot, it is seen that no P-wave arrival was observed below epicentral distance of 24 degrees. Also between epicentral distances of about 90° and 106°, there exists a shadow zone which indicate a low velocity zone for which the applitudes of P-waves are much reduced. Such a shadow zone corresponds to the presence of a discontinuity surface in which the P velocity sharply diminishes from above to below (Bullen, 1985). Other scattered points on the plot may be due to misjudged times, other phases or local cultural events which were picked at random. These points were later found to have very high residuals and were therefore disregarded. Hence, only events with residuals in the range between ±5.0 s were considered for further analysis. This consisted of 110 events shown in Appendix II. All arrival times associated with these events are then plotted in Figure 4.4. A comparison of this plot with the standard travel time plot (Bolt and Nuttli, 1976) shows that P-phases and PKP-phases are more frequently picked at the station.

The number of arrivals reported at the station on yearly basis from 1985 to

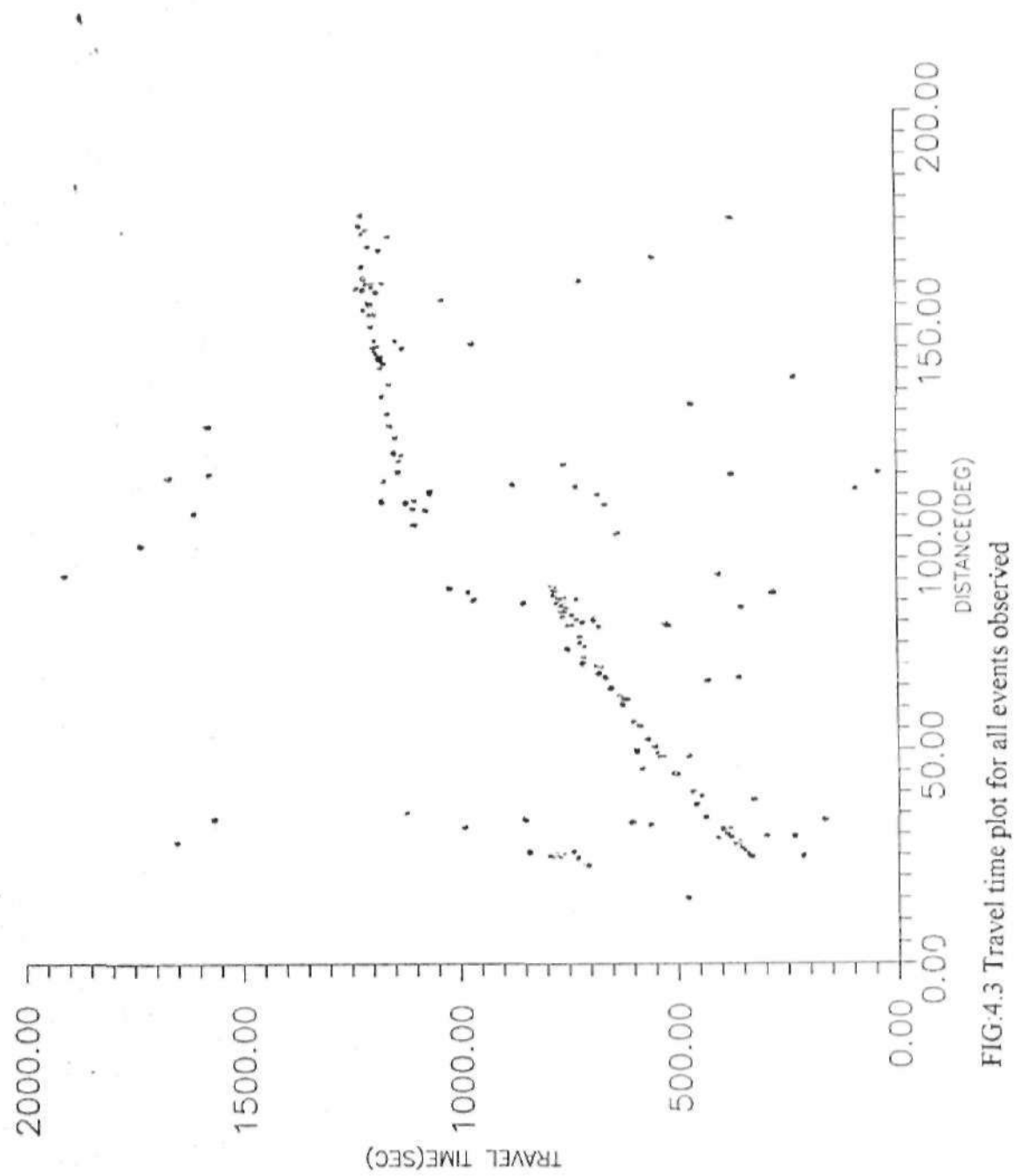

FIG.4.3 Travel time plot for all events observed

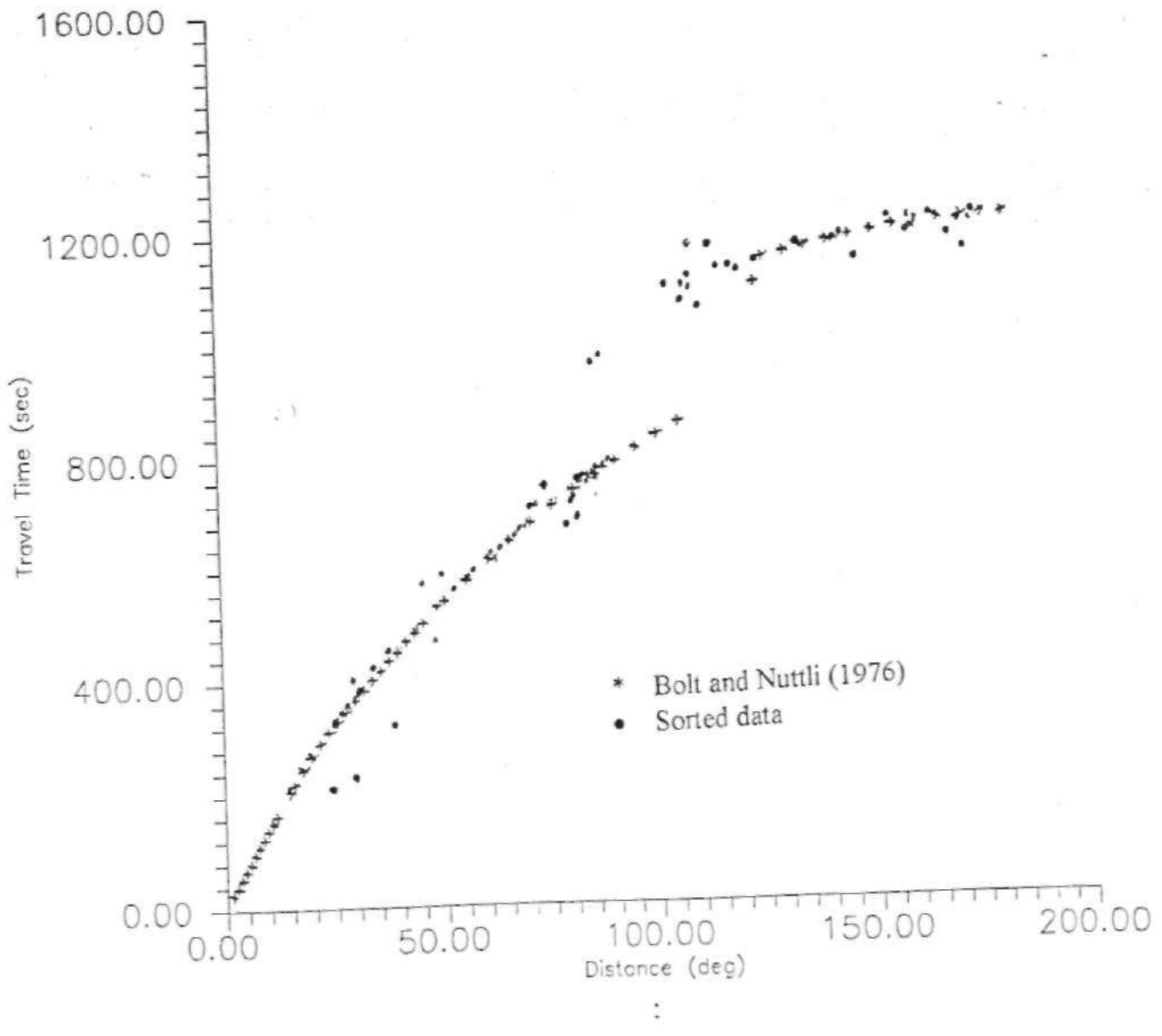

FIG:4.4: Travel time plot for sorted events

1992 is shown in Table I. The number of P and PKP phases are also indicated. The number of events are limited because the station is located on a site with high cultural noise and therefore operates at amplification level which permits only events whose magnitudes are large enough to be picked. Also, the number of events recorded in 1987 and 1991 are low because records of events for some months were not available due to equipment failure. A closer look at Appendix I reveals that only a few events with magnitudes less than 5 were picked, most events have magnitudes higher than 5.

Figure 4.5 displays a frequency distribution of the P-phase travel time residuals placed into 0.1 s bin. This histogram is truncated at ±4.0 s and the height is normalized to the height of the bin with the largest number of picks. The histogram is smoothed (solid) by averaging three adjacent data points (dots). The histogram tend to depart from a Gaussian shape and tend to be positively skewed and have several well pronounced peaks. The positive skeweness is due to the fact that the station is operated at low gain, because of high cultural noise, and therefore, most of the arrivals tend to be delayed (i.e positive residuals).

4.2.2 Azimuthal Variation of Travel-Time Residuals.

Another contribution to the differences in travel-time residuals is azimuthal variation (Bolt and Nuttli, 1976; Herrin and Taggart, 1968; Lilwall and Douglas,

TABLE I : Number of events reporting at the station

YEAR	NUMBER OF ARRIVALS	PHASES
1985	35	P 22 PKP 13
1986	26	P 10 PKP 16
1987	19	P 11 PKP 8
1988	46	P 31 PKP 15
1989	35	P 23 PKP 12
1990	34	P 28 PKP 6
1991	11	P 3 PKP 8
1992	24	P 13 PKP 11

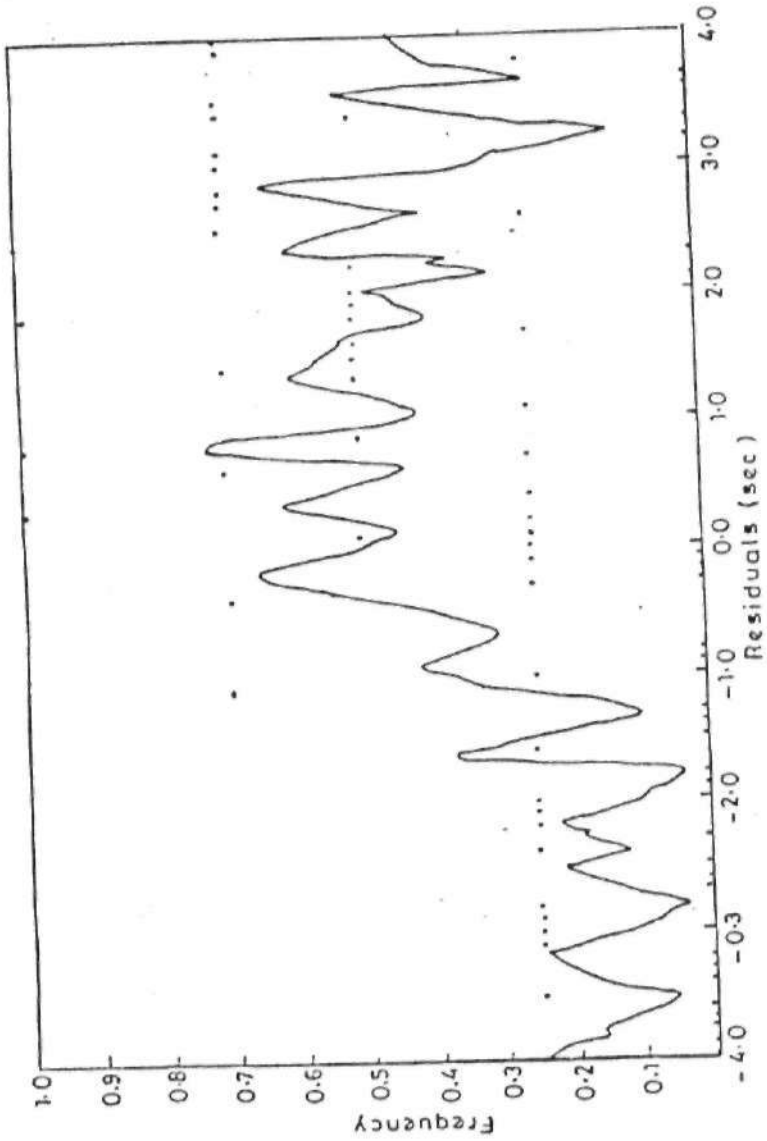

FIG. 4.5: Frequency distribution of P-phases.

1970; Dziewonski and Anderson, 1983). Azimuthal variation can be due to a combination of earth structure near the source and receiver, and upper mantle anisotropy. For example, sources or stations situated in a region of recent tectonics or stable shield will have their residuals influenced by the nature of the structure in that region. By dividing the earth's surface into bins 10° in azimuth by 10° in distance relative to the station, the travel time variation between different source regions was examined. The result of this windowing is shown in Figure 4.6.

In this figure, each concentric ring represents an increament of 30° in epicentral distance and the map is centred on Zaria station. The residuals in each azimuthal bin "i" and distance "j" are averaged for each bin and plotted centered on that bin. The triangles are negative residuals (early arrivals) and the circles are positive residuals (late arrivals). Hatched shading of the symbols indicate that the bin has only one arrival. The new station mean residual was calculated to be 0.72 ± 1.81 s by summing over the average residual for each bin. The large standard deviation of the mean suggests that the variation in the residual cannot be accounted for by considering the data as belonging to one homogeneous set.

The systematic azimuthal biases of the residuals are investigated according to Dziewonski and Anderson (1983). This is shown in Figure 4.7, in which the absolute residuals are plotted against the back azimuth. The scatter observed in the plot is expected because absolute travel time residuals are assumed to be characterised by changes in the propagation paths. Also of importance is that

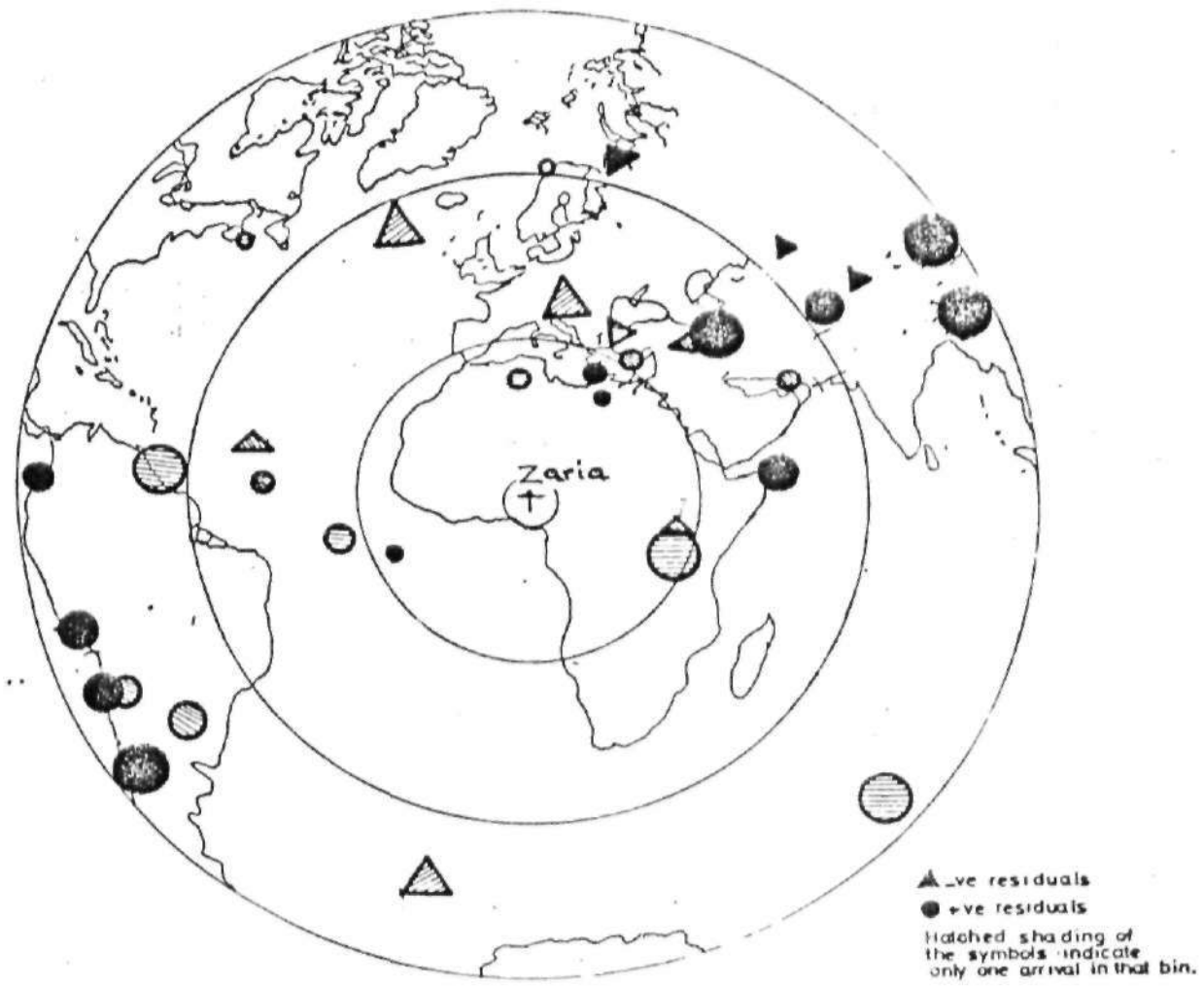

FIG. 4.6: Station residuals centers on Zaria with circles and triangle indicating average residuals centred on 10^0 in azimuth by 10^0 distance bin.

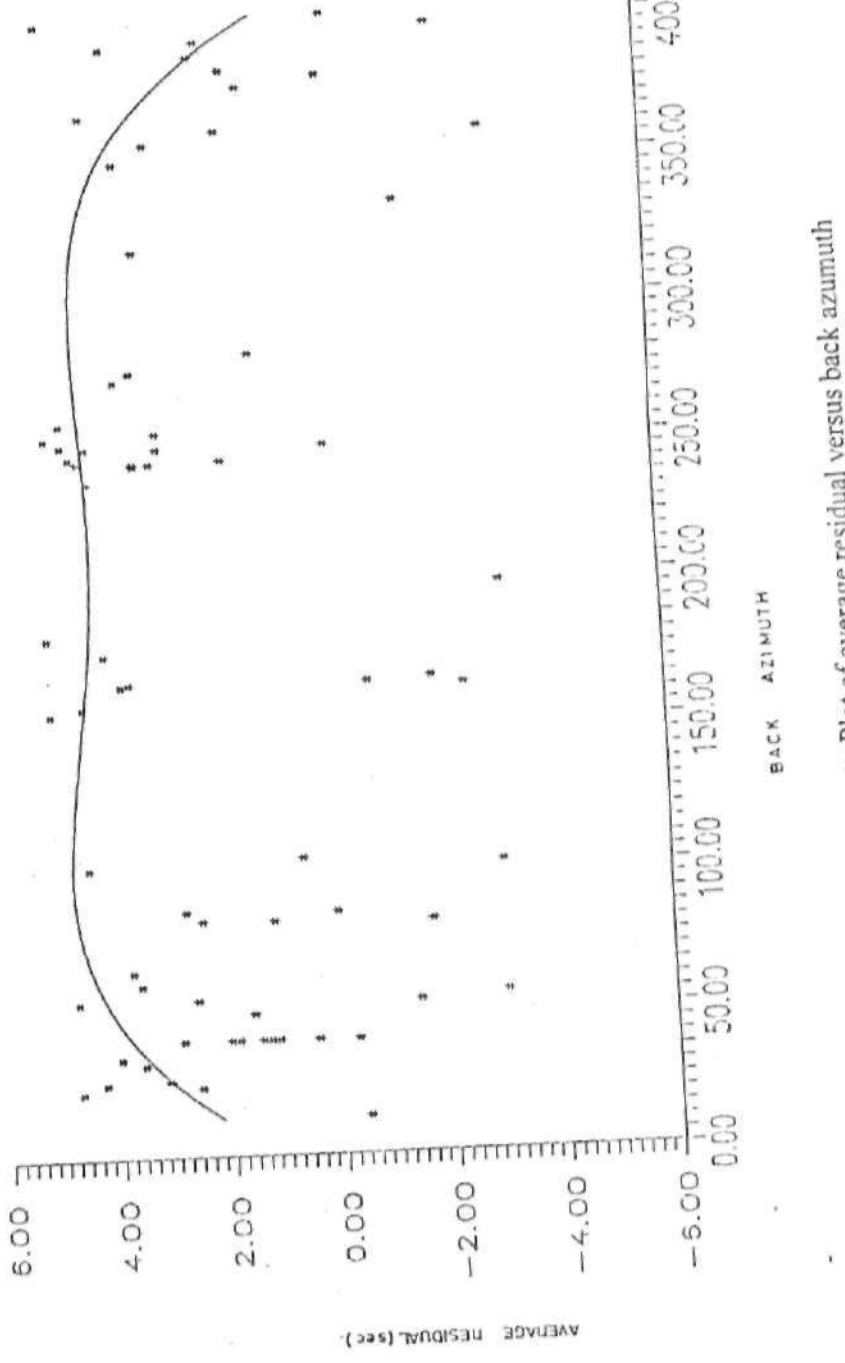

FIG. 4.7: Plot of average residual versus back azumuth

about 80 percent of the residuals lies between ±3.0 s and only 20 percent have residuals up to ±5.0 s. This is an indication that the data set is reasonable. The scatter can be minimized if the average residual of each bin or the relative residuals was plotted. The effect of these plots could not be investigated because of the fact that the data set available is few. A least square fit (Agarwal et al.; 1976; Dziewonski and Anderson, 1983) with a constrained fourth order polynomial was fitted to the data.

The average of all residuals i.e the station mean residual and the average of the average residual for each bin, which are referred to as residuals before and after sorting respectively (Lorrain and Clayton, 1991) reveal a positive mean residual for the station, which indicate that most of the events arriving at the station are delayed. Explanation for this is that the station is operated at low gain, and low gain stations report late arrival times (Grand, 1990). Also, the station is located in a region of recent tectonics (Pan-African Orogeny 550 ± 100 m.y.), and the general world-wide law of tectonics (Vitorello and Pollack, 1987) reveals a generally decreasing heat flow with tectonic age. Therefore, it is expected that the temperature regime of the upper mantle must be hotter than for normal upper mantle.

Comparing the station residual plot for Zaria (Fig.4.6) with residual plot for stations such as AAE (Addis-Ababa, Ethopia) Fig. 4.8, LWI (Lwiro, Zaire) Fig. 4.9, KIC (Kosan-Boka, Cote D' voire) Fig. 4.10, and NAI(Nairobi, Kenya) Fig. 4.11, it is

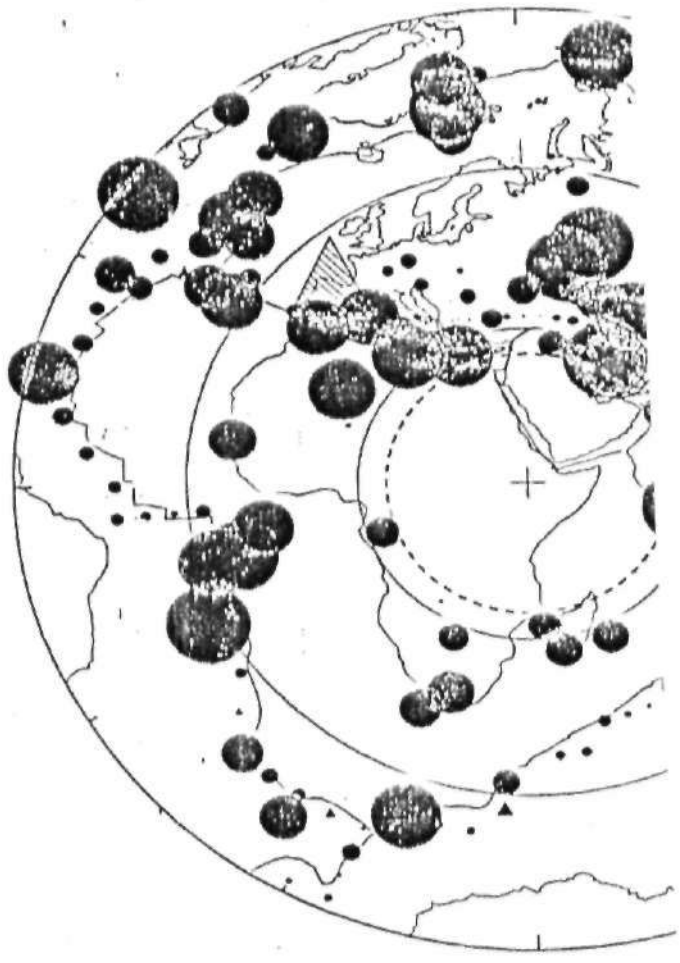

FIG. 4.8: Residual plot of AAE (Addis-Ababa) ex
(After, Lorrain and Clayton, 1991)

FIG. 4.9: Residual plot ofLWI (Zaire) extracted from
(After, Lorrain andClayton, 1991)

FIG. 4.10: Residual plot of KIC (Kosan-Boka
(After, Lorrain and Clayton, 1991)

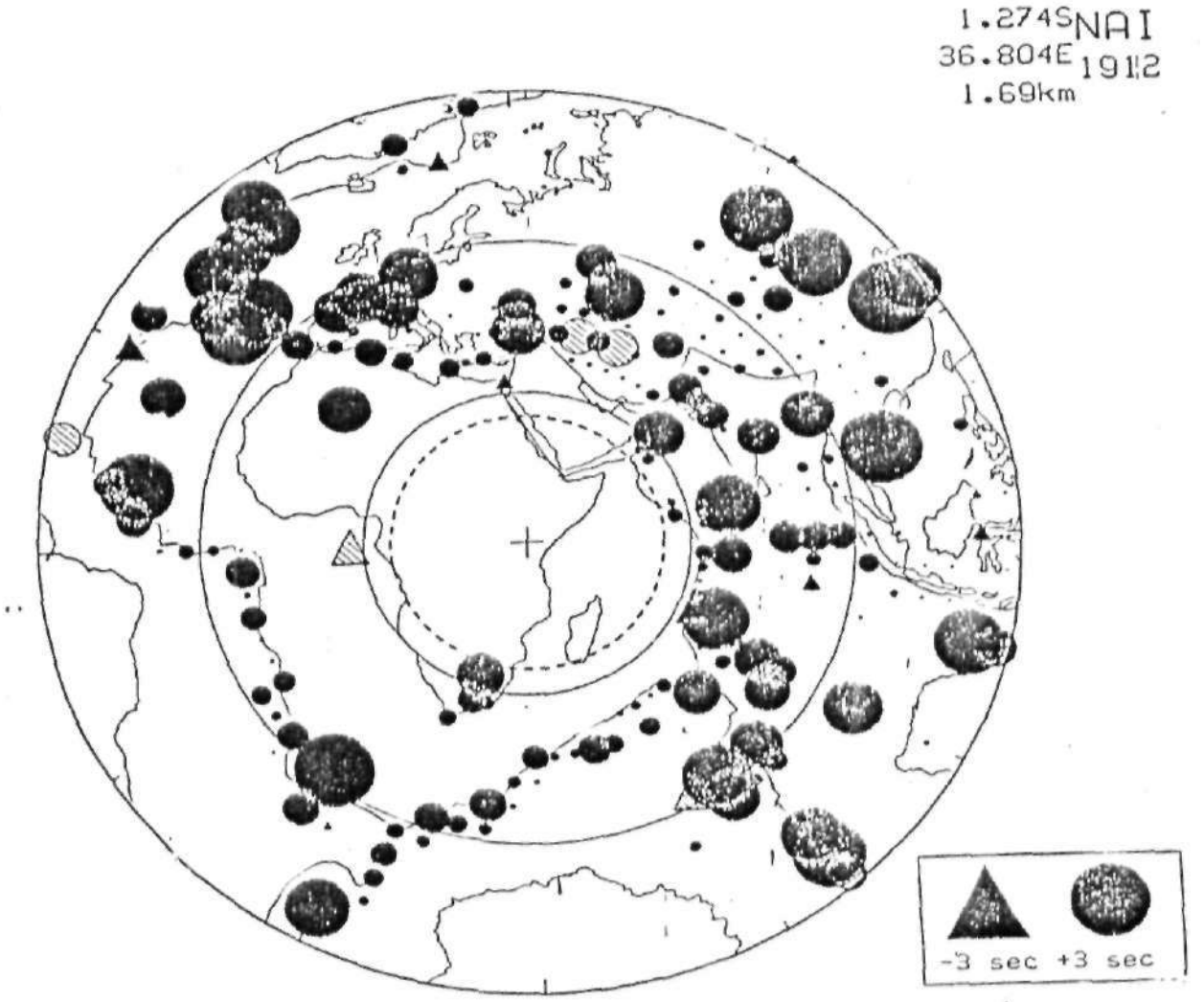

FIG. 4.11: Residual plot of Nairobi (NAI) extracted from ISC Bulletin (After, Lorrain and Clayton, 1991)

observed that stations such as AAE, LWI, and NAI located in a region with high seismicity (around and within the East African rift valley) all reported late arrivals i.e positive residuals, while KIC located in the stable West African craton reported early arrivals i.e negative residuals. This shows good correlation with the result observed for Zaria station.

4.2.3 Relative Residuals

The absolute travel time residuals are made up of contributions from the source region, propagation path and station region, except at large epicentral distances when the source and station effects become small compared to the propagation path effect.Azimuthal contributions to the absolute travel time residuals were examined in section 4.2.2. As earlier observed (Fig.4.7), there is a large scatter in the values of the absolute travel time residuals due to changes in the propagation paths. Consequently, in order to minimize the observed scatter in the absolute residuals, it is therefore imperative that the contributions be reduced to that of the station region only. To achieve this, relative residuals of some events listed in Appendix III are computed relative to a reference station (Zaria) for a group of stations in Senegal, Cote D'Ivoire, Ghana, Cameroon, Central African Republic, Zaire and Kenya. The choice of Zaria as reference station is due to its central location in the group. Therefore, the contribution to the residual is reduced to the contribution due to lateral variation in the crust or upper mantle structure in the station region only.

Appendix III summarizes the absolute and relative travel time residuals for the stations and events selected for the study. The events are located in five different regions; North Ascension, Burma/India/China, East Kazakhstan, South and Central America and the Mediterranian regions (Greece, Eagean sea, coast of Libya, Ionian Sea and East Mediterranian).

A closer look at the table reveals that events from Mediterranian region have early arrivals in most of the stations except for stations in Cameroon and Kenya. The mean relative residual for this region is -1.76 ± 0.91 s. Events from South and Central America also show a negative relative residual with a mean of -1.93 ± 0.79 s for all the stations in West and Central Africa, but have a positive residual for the station in Kenya. Also, events from North Acension indicate negative residuals at all stations in West and Central Africa, with a mean residual of -2.9 ± 3.5 s. The large mean relative residual and large standard deviation of events for this region is due to the high values of the absolute residuals reported by the reporting station to ISC. Events from East Kazakhstan have positive relative residuals with a mean of 0.55 ± 0.41 s, while events from India/Burma/China give negative relative residuals for all stations in West and Central Africa with a mean of -1.804 ± 0.76 s.

The trend of the relative residuals indicate lateral inhomogeneity of the crust and upper mantle between the various stations and Zaria station; in which case the relative residuals are highly dependent on the direction of approach of the P-waves (Bolt and Nuttli, 1976).

The station in Senegal (KDS) located in the Taoudeni basin of the stable West African Craton recorded only 2 of the 30 events and has negative residuals for the events, while all the stations in Cote D'Ivoire and Ghana (except LEGH in Accra) are located in the Leo shield of the West-African Craton. These stations recorded almost all the events and in most cases reported early arrivals (negative relative residuals). Stations in Cameroon (KBC and EKC) are located around the active volcanic region of Cameroon, only two of the events were recorded by the stations and these indicate late arrivals (i.e positive relative residuals). Other stations in Central Africa Republic and Zaire are located in the Congo Craton and in most cases reported negative relative residuals for almost all the events. The station in Kenya (NAI), located within the East African rift which may be an extremely anomalous region in terms of seismic structure (Grand, 1990) have positive relative residual for almost all the events recorded at the station. However, there is no information as to the properties of the seismographs in terms of band pass and magnification for the stations, except NAI (Kenya) which is operated with station amplification of 50 K.

Zaria station (Nigeria) is located on the eastern flank of the West-African Craton in a region affected by the Pan African Orogeny. The partial melting of the thickened crust which resulted from the collision at the cratonic margin (Burke and Dewey, 1972; Trompette, 1979) forming granitic magma, the so-called older granite (Ajibade et al.; 1979), forms the basement rock. Therefore, there results a steep thermal gradient extending through the Southern sector of the belt (Ghana - Togo -

Benin), and a long way under the Dahomeyan shield and as far east as Nigeria (Grant, 1969). As a result, the temperature regime of the crust and upper mantle in this region is expected to be hotter than for other stations in West and Central Africa located within the stable West African Craton and the Congo Craton.

4.3 VELOCITY - INVERSION

The observed travel time data form a discrete set of points from which it is required to find the (V,Z) plane (V being the velocity and Z the depth), the closed area which contains all velocity-depth curves corresponding to the observed data. The method is based

on the use of tau (p) method of Bessonova et al.(1976) for deriving extremal bounds on possible velocity models described in Chapter Three. However, it is important to investigate the azimuthal distribution of events so as to ensure that data set belong to a uniform geologic region. This is necessary for a meaningful result. Fig. 4.12 shows the azimuthal distribution of events with respect to the epicentral distance, while the insert shows the distribution in polar coordinate. Shaded portion shows that more events occurred in the continental region than in the other regions, therefore, inversion was attempted for this region. The corresponding travel time versus distance curve is shown in Fig. 4.13.

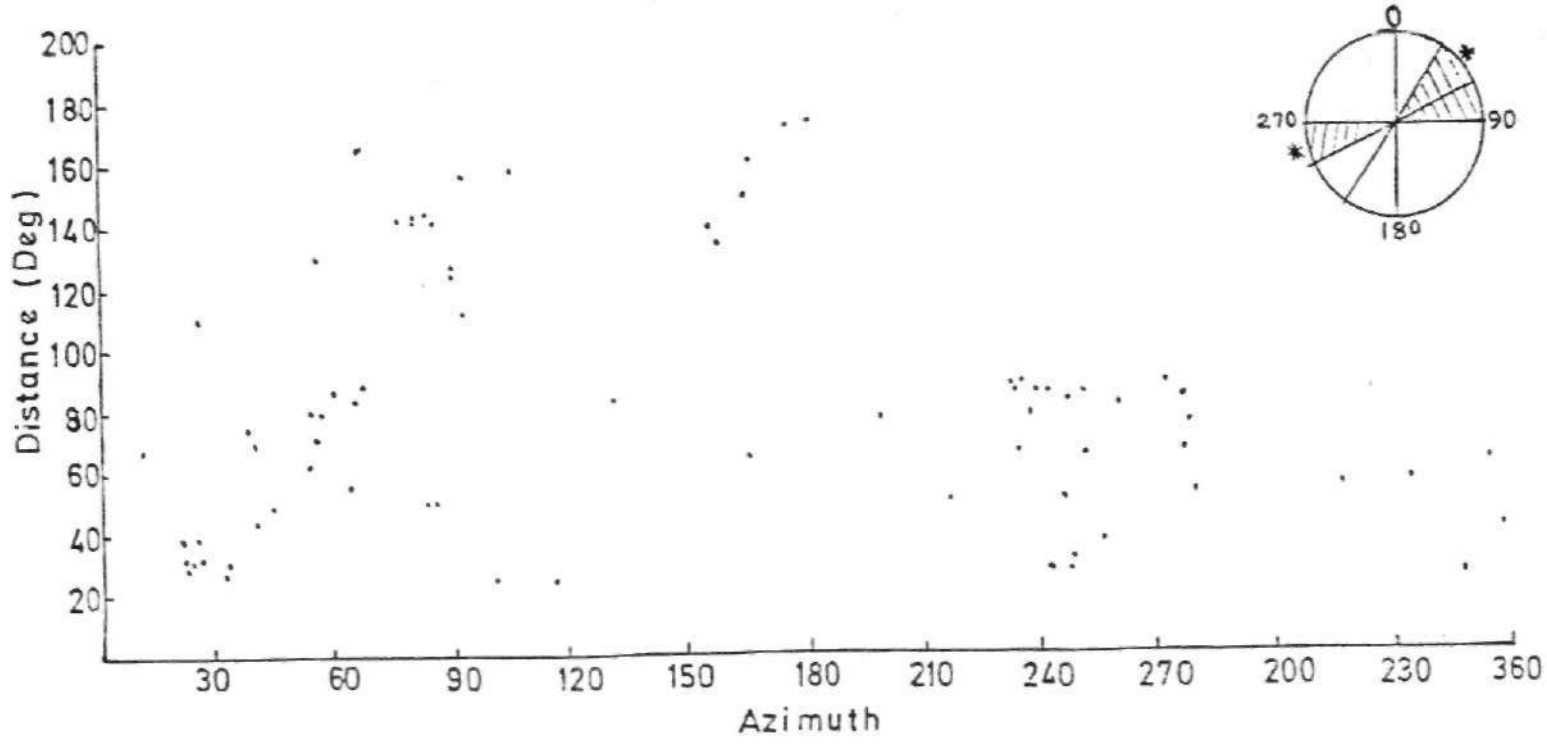

FIG. 4.12: Azimuthal distribution of events versus distance (Deg)
(Insert; Azimuthal distribution in polar co-ordinate)
* high occurrence of Earthquakes

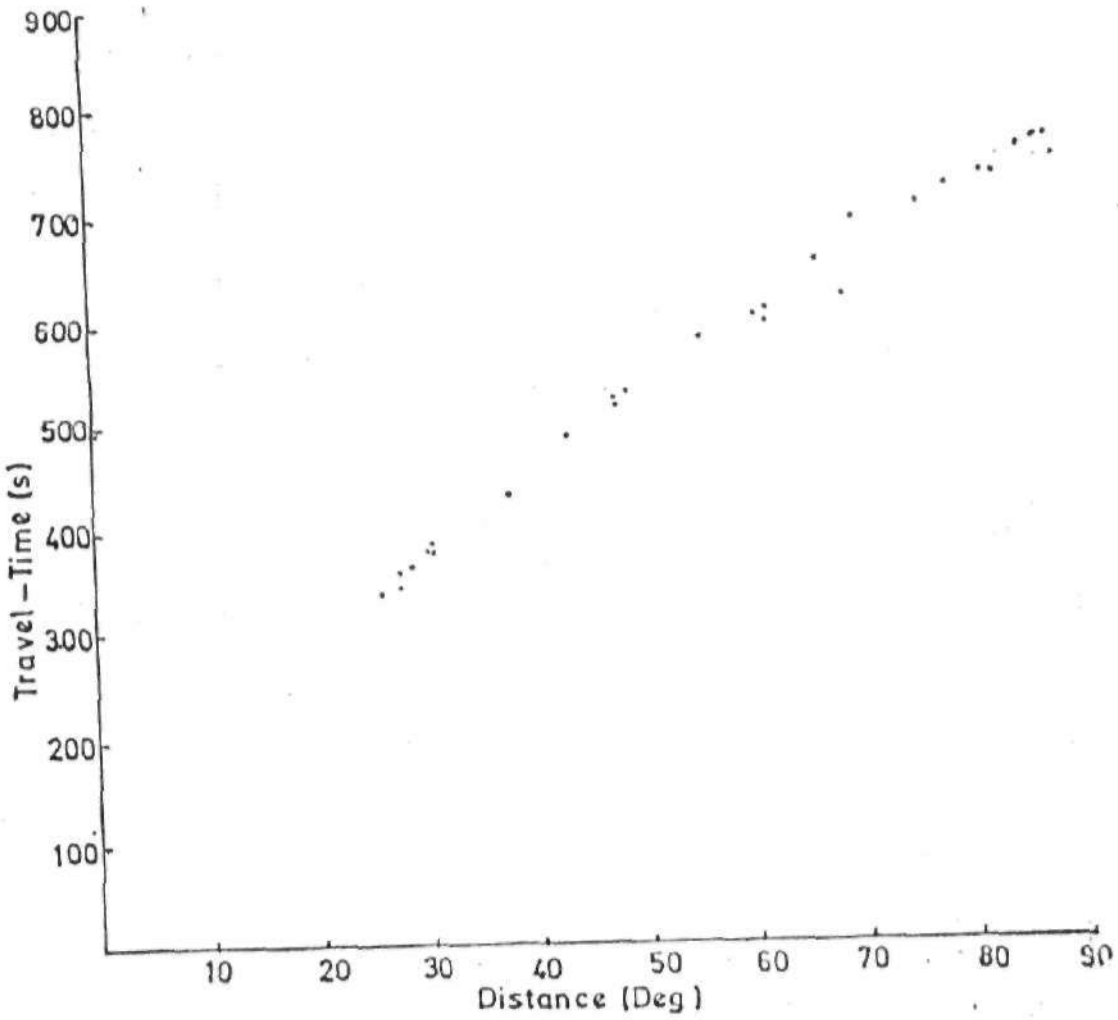

FIG. 4.13: Plot of time-distance curve for continental region.

By assuming trial values of p, a reduced travel time plot (Fig. 4.14) was plotted. The figure shows that due to the relatively few data available, the maximum of the curves are not clearly defined, and the tau does not have a clearly defined value. Hence, the inversion of the data will be difficult. It is therefore suggested that in order for the inversion to be properly carried out, it is necessary to gather more data for at least another 10 years.

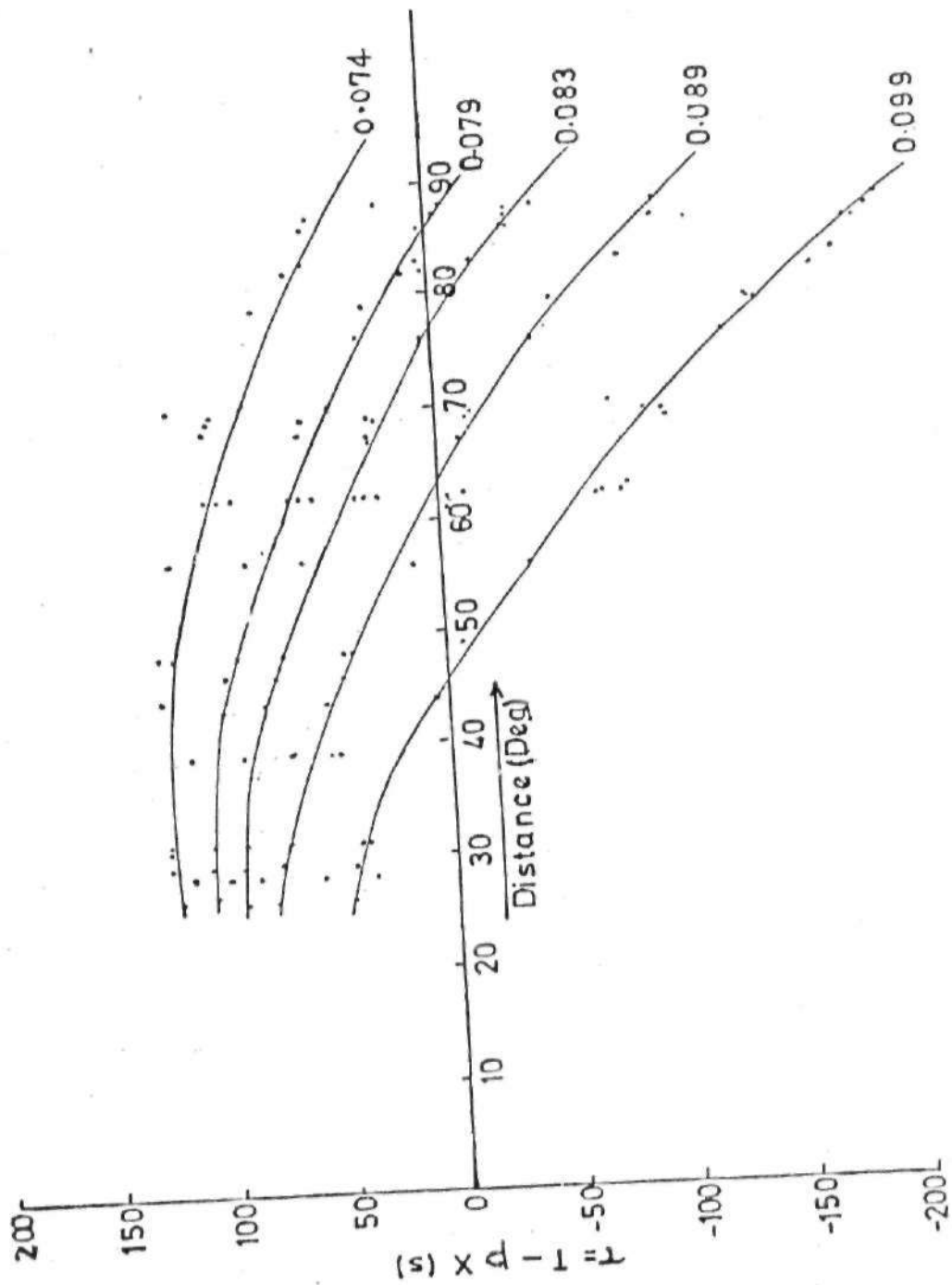

FIG. 4.14: Plot of reduced travel-time versus distance

CHAPTER FIVE

DISCUSSION AND CONCLUSIONS

The events recorded at the A.B.U. station all lies within the epicentral distance of about 24° and 180°. Only events with magnitude of 5 and higher were recorded. This result is summarized in Appendix I and their locations plotted on Figure 4.2 in equidistant azimuthal projection centred at Zaria. The events spread across five major tectonic regions; the Mediterranean, East Kazakhstan, Burma/India/China, North Ascension and South and Central America. Only a few events are recorded from other regions and Africa. The tectonics along the travel paths of these events affect the amplitude of their residuals. The hotter the travel-path region the higher the delay in travel times.

The Mediterranian events have a mean absolute residual of 1.05 ± 0.85 s; the paths bottom beneath the African plate through the Hoggar shield in North Africa, a region in the eastern flank of the stable West African craton affected by the Pan-African Orogeny. The collision at the cratonic margin, resulting in steep thermal gradient in the crust probably caused the delay in travel times. For the Kazakhstan events with a mean negative absolute residual of -0.9 ± 0.4 s, the travel paths bottom in the upper mantle region beneath the eastern Mediterranean, Coast of Turkey, Syria and Lebanon. The processes taking place in this region involve a collision of the African plate and the Eurasian plate and also movement between

the small Aegean and Turkish plates (Mckenzie, 1970) which involve the consumption of the Mediterranean Sea floor. This could well lead to the presence of high velocity slabs in the upper mantle resulting in the faster travel paths (negative residual) for this region. For the Burma/India/China events with a mean absolute residual of +2.33 ± 1.18 s, the travel paths bottom beneath the Red Rea and the Arabian plate, while the South American and the North Ascension events with a mean absolute residual of +1.4 ± 1.0 s and +0.2 ± 0.7 s respectively, bottom beneath the Mid-Atlantic region. The Red Sea region and the Mid-Atlantic which also exhibit positive residuals are active spreading centres. The spreading rate in the Mid-Atlantic estimated at an average of 2.0 cm/year (Minster et al.; 1974) is twice the value of 1 cm/year estimated on the axis of the Red Sea (Mckenzie et al.; 1970), which explains why the positive residuals for paths beneath the Red Sea is higher than those for paths beneath the Mid-Atlantic ridge.

Therefore, the mean absolute residual of +1.08 ± 2.1 s observed for the station is expected considering the various paths traversed by events recorded at the station. Also the large standard deviation of the mean suggests that the variation in the residual cannot be accounted for by considering the data as belonging to one homogeneous set. Other factors which could have contributed to the delay in travel times include the operational low band pass (3-5 Hz) and operational low gain of the station . According to Grand (1990) low gain stations reports systematic late arrivals.

In order to minimize the scatter in the absolute travel time residual, the residual data was sorted into bins, 10° in epicentral distance by 10° in azimuth. The new station residual after sorting is 0.72 ± 1.81 s, which is different from the result obtained before sorting (1.08 ± 2.1 s) and has less scatter. Also the effects of travel paths and source on the residual are removed from the absolute residual. Thus, reducing the effect on the residual to that of the station region only. Looking at Appendix III, events from Mediterranean, India/Burma/China, South America and North Ascension Island which hitherto have mean positive residual now have negative relative residuals with respect to the Zaria station, and the Kazakhstan events now has positive relative residual. The reason for this might be due to the fact that some stations which record most of the events considered are located in the stable West-African craton and Congo craton compared to Zaria which is located in the Pan-African mobile belt.

An inversion of the travel time data was attempted using the tau method (Bessonova et al.; 1974, 1976), but because of the relatively few data available it was not possible to properly carry out the inversion. It was therefore recomended that more data must be gathered for, at least, another ten years.

In conclusion, this study has shown that patterns of travel time residual are a good indicator of the upper mantle structure underneath a station. The mean absolute residual of the station before and after sorting was found to be positive i.e generally delayed, which indicate that the station region may not be quite stable.

The relative residuals suggests that the temperature regime of the upper mantle in the Zaria region is hotter than for other regions in the stable West African Craton and Congo Craton. The tectonic process taking place in the region involves the partial melting of the emplaced granitic magma, the so called older granite which forms the basement rock.

REFERENCE

Adeniyi, O.O., Osazuwa, I.B., Ojo, S.B., (1992). A gravity study of the older granite suite in Zaria area of Kaduna state, of Nigeria Journal of Mining and Geology vol.,28 No 2:56-60.

Affaton, A. (1975). Etude geologique et structural du nordouest Dahomey Nord Togo et du Sud-East de la Haute-Volta. Trav Lab Sci. Terre Saint-Jerome, Marseille, Bio: 201.

Agarwal, N.K., Jacoby, W.R., and Berkhemer, H., (1976). TeleseismicP-wave travel time residuals and deep structure of the Aegean region. Tectonophysics, 31: 33-57.

Ajakaiye, D.E., Ojo, S.B., Daniyan, M.A., and Abatan, A.O., (1989). (Editors). *Proceedings of the National Seminar on Earthquakes in Nigeria*

Ajakaiye, D.E., Daniyan, M.A., Ojo, S.B., and Onuoha, K.M., (1987). The July 28, 1984 South-western Nigeria Eathquake and its implications for the understanding of tectonic structure of Nigeria. Journal of Geodynamics, 7, Pg. 307-317.

Ajibade, A.C., Fitches, W.R., and Wright, J.B. (1979). The Zungeru mylonites, Nigeria recognition of a major tectonic unit. Rev. Geol. Dyn Geogr Phys, 21 (5) : 359-363.

Bakus, G., and Gilbert, F. (1968). The resolving power of gross earth data. Geophysics J.R. astr. Soc., 16: 169-205.

Ballard,S., and Pollack, K. (1987). Diversion of heat by Archean Cratons: a model for Southern Africa. Earth plane Science letters 85: 253-264.

Barre're, J. (1976). Le groupe precambrien de L'Ansaga entre Atar et kjoujt (Mauritanie). Etu d'un metamorphisme profound et de ses relations avec la migmatisation. Mein Bur Rech Geol Min., 42: 275.

Bath,M. (1979). Introduction to Seismology. 2nd revised edition. Basel:- Birkhauser Verlag.

Bertrand and Caby, R. (1977). Geodynamic evolution of the Pan-African Orogenic belt: a new interpretation of the hogger shield. Geol. Rundsch 67: 357-388.

Bessoles, B. (1977). Geologie de la Afrique. LeCraton Quest Africain. Mem. Bur Rech Geol Min, Paris 88: 402.

Bessonova, E.N., Fishman, V.M., Ryaboyi, V.Z. and Situikova, G.A. (1974). The tau method for inversion of travel times-I. Deep seismic sounding Data. Geophys .R. astr. Soc. 36: 377-398.

Bessonova, E.N., Fishman, V.M., Shnirman, M.G. and Situikova, G.A. (1976). The tau method for inversion of travel times-II. Earthquake data. Geophys. J.R. astr. Soc.46: 87-108.

Black, R., and Caby, R. (1979). Evidence for late Precambrian Plate tectonics in West- Africa. Nature 278: 223-227.

Bolt, B.A. and Nuttli, O.W. (1976). P-wave residuals as a function of azimuth. J. Of Geophys Res., 71: 5977-5985.

Briden, J.C., Whitcombe, D.N., Stuart, G.W., Fairhead, J.D., Dorbath, C. and Dorbath, L. (1981). Depth of geological contrast across the West-African craton margin. Nature (Lond) 292: 123-128.

Bullen, K.E. (1985). An Introduction to the theory of seismology (5thEd.). Cambridge Univ Press, London and New York.

Burke, K.C. and Dewey, J.F. (1972). Orogeny in Africa. In: Dessauvagie TFJ, Whiteman A.J (eds) African Geology. Depth. Geol Univ. Ibadan, Nigeria, Pg 583-608.

Caby, R. (1987). The Pan-African belt of West Africa from Sahara Desert to the gulf of Benin. "The anatomy of the mountain ranges." Scher J.P., and Rodgers, J. (eds). Princeton Univ. Press U.S.A.

Caen-Vachette, M. (1988). Le Craton Quest-Africain et le boucher guyanais:Un seul Craton au Proterozoic inferieur? Jour. Africa Eearth Science 2: 218-225

Cliford,T.N. (1970). "The structural framework of Africa".African Magmatism and Tectonics. Hafner Publishing Company, N.Y.

Dorbath, C. and Dorbath, L. (1984). Approche seismologique de la structure de la lithosphere en Afrique de l'Quest. Th'ese Univ, Paris VI, pp 307.

Dorbath, C., Dorbath, L., Le page, A.M. and Gauloh, R. (1983). The West African Craton margin in Eastern Senegal: a seismological study. Ann. Geophysics 1:25-36.

Dorbath, L. and Montaguer, J.P. (1983). Upper mantle heterogeneity in Africa deduced from Rayleigh wave dispersion. Phys; Earth planet; Inter. 32:218-225.

Dziewonski, A.M., and Anderson, D.L. (1984). Travel times and station corrections for P-wave at teleseismic distances. J. Of Geophys; Res. 88: 3295-3314.

Engdahl, E.R, Sindorf, J.G. and Eppley, R. A. (1977). Intepretation of relative teleseismic P-wave residuals. J. of Geophys. Res. 5671-5682.

Grand, S.P. (1990). A possible station bias in travel time maesurements reported to ISC. Geophy. Res. letters, 17: 17-20.

Grant, N.K. (1969). The late Precambrian to early Palaeozoic Pan-African Orogeny in Ghana, Togo, Dahomey, and Nigeria, Geol. Soc. Amer., Bull. 80: 45-56.

Gregersen, S. (1977). P-wave travel time residuals caused by a dipping plate in the Aegean Arc in Greece. Tectonophysics, 37: 83-93.

Hardiouche and Jobert, (1988). Geographical distribution of surface wave velocities and B-D upper mantle structure in Africa. Geophys. Jour. 95: 87-109.

Herrin, E.,and Taggart, J. (1968). Regional variations in P-wave travel times, Bull, Seismol. Soc. Am. 52: 1325-1337.

Ige,E.A. (1984). December 21, 1975 tremor near Fagwalawar Garu in Dambatta, Kano. Unpublished Research.

Jeffreys, H. and Bullen, K.E. (1970). Seismological Tables. British Association for the advancement of Science, Gray Milne Trust.

Johnson,L.R. and Gilbert, F. (1972). Inversion and inference for a teleseismic ray data, in: Methods in computational Physics, edited by Bolt , B.A., 11:231-266.

Kennedy, W. (1964). The structural differentiation of Africa in the Pan-African (+500 m.y) tectonic episode. 8th Ann. Res. Inst. Afr; Geol, Leeds Univ. U.K.

Kennett, B.L.N. (1976). A comparison of travel time Inversions. Geophys. J.R. astro. Soc., 44: 517-536.

Kennett, B.L.N. and Orcutt, J.A. (1976). A comparison of travel time inversions for marine refraction profiles. J. Geophys. Res., 81: 4061-4070.

Le blanc (1976). Proterozoic oceanic crust at Bou Azzer. Nature (Lond) 261: 34-35.

Lilwall, R.C., and Douglas, A., (1970). Estimations of P-wave travel times Using the joint epicenter method. Geophys. J.R. Astro. Soc. 19: 165-181.

Lorrain, J.H. and Clayton, R.W., (1991). A station catalog of ISC arrivals: Seismic station histories and station residuals. Publ. by United State Geological Surveys.

McCurry, P. (1970). The geology of Degree sheet 21 (Zaria). Msc. Thesis, Ahmadu Bello Univ., Zaria.

Mckenzie, D.P. (1970). Plate tectonics of the Mediterranean region. Nature, 226: 239-243.

Mckenzie, D.P., Davis, D and Molnar, P. (1970). Plate tectonics of Red Sea and East Africa. Nature, 226: 243-248.

McMechan, G.A. and Wiggins, R.A. (1972). Depth limits in body wave invertions. Geophys. J., 36: 541-576.

Minster, J.B., Jordan, T.H., Monlar, P. and Haines, E., (1974). Numerical modelling of instantaneous plate tectonics. Geophy. J., 36: 541-576.

Morgan, W.J. (1971). Convection plumes in the lower mantle. Nature, 230: 42-43.

Morgan, W.J. (1972). Plate motion and deep mantle convection. Geol. Soc. Am. Mein., 132: 7-9.

Odeyemi, J.B., (1978). Preliminary report on the field relationships ofthe basement complex rocks around Igarra, Mid-West In: C.A. Kogbe (Editor), Geology of Nigeria Elizabethan Publ., Lagos pp. 59-63.

Ojo, S.B. (1994). Teleseismic P-wave travel time residuals at the Ahmadu Bello University seismic station, Jour. Of Mining and Geology Vol. 30, No. 1 75-80.

Panagoitopoulos, D.G., Hatzidimitroic, P.N., Karakaisis, G.F., Papadimitrou, E.E.,and Papazachos, B.C. (1985). Travel time residualsin South-eastern Europe, PAGEOPH.vol. 123.

Reichelt, R., (1972). Geologie du Gourma. Mem Bur Rech Geol Min, Paris 53 pp 213.

Ritz, M. and Robnean,B. (1976). Crustal and upper mantle electrical conductivity structures in West Africa: geodynamic implications. Tectonophysics 124: 115-132.

Rocci, G., Bronner, G. and Deschamp, (1991). " The West African Orogens and circum-Atlantic Correlatives". Crystalline basement of the West African Craton. Springer-Verlag Berlin Heidelberg, N. Y. Pg. 31-61

Roussel, J. and Lesqoer, A., (1991). "The West African Orogens and circum-Atlantic Corrlatives". Geophysics and crustal structure of West Africa. Springer-Verlag Berlin Heidelberg, N. Y.

Trompette, R., (1979). Les Dahomeyides du Benin, Togo et Ghana: une chaine de collision d'age Pan African. Rev. Geol Dyn Geogr Phys 21: 339-349

Vachette, M., Rocci, G. and Sougy, J., (1975). Ages radiometriques Rb\Sr de

2000 a 1700 m.a de series metamorphiques et granites intrusifs Precambriens de la partie N et NE de la dorsale Reguibat (Mauritanie Septentrionale) 7 eme Colloque International de Geologie Africaine, Fiorence. In: Trav. Lab. Sci. Terre St Jerome, Marseille, B 11: 142-143

Vitorello, I and Pollack, H.N., (1987). Diversion of heat by Archean cratons: a model for Southern Africa. Earth Planet Sci. Letters 87: 253-264.

Webb, P.K., (1972). Recent Research on the Geology between Zaria and Kaduna. Savannah, Vol. 1 No. 2, Pp 241-243.

APPENDIX I: LIST OF ALL SELECTED EVENTS

s/no	date	lat(deg)	long (deg)	Origin time (h m s)	Arrival time (h m s)	region	magnitude	depth (km)
001	100185	12.830	-86.180	240922	244056	NICARAGUA	4.4	91
002	100185	10.797	-43.446	174755	175652	N.ATLANTIC	5.8	10
003	180185	-29.374	-70.793	150009	151239	CENTRAL CHILE	5.7	83
004	210185	-0.953	128.507	005522	011415	HALMAHERA	5.8	33
005	260185	-33.053	-68.467	030657	031934	ARGENTINA	6.0	05
006	310185	-46.083	165.092	043257	045224	OFF W.COAST	5.8	10
007	100285	49.877	+78.816	032707	033819	EASTERN KAZAKH	5.9	-
008	270285	-1.316	-14.568	225740	230307	N. OF ASCENSION	4.9	10
009	050385	35.547	+1.436	153755	154321	ALGERIA	5.0	10
010	190385	-33.198	-71.653	040108	041350	NEAR COAST OF C. CHILE	5.9	42
011	210385	56.523	-34.404	235440	000416	NORTH ATLANTIC	5.1	10
012	130485	+1.622	126.411	030006	031848	MOLUCCA PASSAGE	5.4	51
013	200485	+9.004	-77.460	182348	183612	NORTH COLOMBIA	5.6	38
014	230485	15.344	120.610	161512	163319	PHILIPINE	6.3	188
015	250485	49.924	+78.969	005706	010816	EAST. KAZAKH	5.9	0
016	300485	39.266	+22.810	181412	182021	GREECE	5.5	27
017	060585	-37.498	179.452	171002	172952	E. N. ZEALAND	5.8	30
018	100585	-5.599	151.045	153550	155524	NEW BRITAIN	6.3	27
019	050685	56.957	+33.748	014142	015120	N. ATLANTIC	5.1	10
020	060685	-4.646	153.173	230458	232427	NEW IRELAND	5.6	68
021	060685	0.952	-28.432	024002	024728	C. M. ATLANTIC	6.3	10
022	060785	-33.430	-72.270	035023	040713	CENTRAL CHILE	~	10
023	290785	36.190	+70.896	075444	080452	HINDU KUSH	6.6	99
024	020885	36.174	-70.780	074658	075700	HINDU KUSH	6.1	120
025	070885	37.445	+21.235	102050	102726	S. GREECE	5.3	31
026	260985	-34.693	-178.656	072751	074456	S. OF KERMADEC	6.3	52
027	200985	-9.829	159.854	033908	035845	SOLOMON IS.	6.2	10
028	051085	62.237	-124.266	152402	155241	CANADA	6.5	32
029	241085	-31.386	-68.605	014855	020253	ARGENTINA	5.7	110
030	251085	52.072	-171.350	012227	013450	ARGENTINA	6.3	112
031	311085	-28.692	-63.171	214920	220136	ARGENTINA	5.6	33
032	071185	-35.257	-179.347	191231	193217	E. N. ZEALAND	5.8	596
033	161185	-38.577	78.368	041218	042446	MID INDIAN RISE	6.2	44
034	281185	-14.043	166.240	022542	024600	VANUATU ISL.	5.8	10

035	2811185	-13.987	166.185	0349954	041010	VANUATU ISL.	6.0	33
036	1501086	-21.777	170.102	2017442	203700	LOYALTY IS.	6.2	150
037	1404686	-13.923	166.831	242512	244510	VANUATU IS	6.0	29
038	2404686	-35.211	-70.637	0710042	072647	CHILE-ARG. BOARDER	4.2	33
039	2604686	57.954	-151.473	0351126	043236	KODIALA IS	3.9	109
040	2105686	+1.929	+99.023	0244444	025116	N. SUMATERA	4.8	128
041	1106686	10.597	-62.928	134601	135904	VENEZUELA	6.0	19
042	2406686	-4.448	143.943	031130	033034	NEW GUINEA	6.6	102
043	2406686	-0.085	-17.824	065654	075243	N. OF ASCENSION	5.7	22
044	0608086	-18.868	169.150	201534	205802	VANUATU IS.	5.5	217
045	1009086	-16.062	-172.888	103442	104044	SAMOA IS.	4.8	33
046	1109086	-5.187	152.442	241825	243700	NEW BRITAIN	5.9	215
047	1309086	-31.827	-179.937	151721	153654	KARMADEC IS	6.0	11
048	1309086	37.014	+22.176	172431	173032	S. GREECE	4.7	47
049	1409086	7.121	-77.105	221220	221803	PANAMA-COLOM. BOARDER	6.5	45
050	1609086	19.376	146.347	182017	163923	MARIANA REG.	5.8	10
051	1709086	10.497	56.983	212516	213400	CHRISEBERG RIDGE	4.6	33
052	2709086	-15.240	-173.800	000235	010025	TONGA ISLAND	4.5	154
053	2709086	-5.370	145.050	074500	074843	NEW GUINEA	5.1	76
054	1410086	-5.058	153.605	175649	182345	NEW IRELAND	-	10
055	2110086	51.264	15.667	043624	051329	POLAND	5.6	49
056	2604086	-5.680	154.051	005923	011901	SOLCMON ISLAND	6.4	138
057	3010086	-22.702	-176.616	012864	014842	FIJI ISLAND	6.3	34
058	1421186	28.901	121.574	212010	213619	TAIWAN	5.6	158
059	2211486	-26.268	167.364	176038	174803	VANUATU ISLAND	6.2	75
060	2903566	33.377	26.265	183637	184300	KERMADEC I	6.0	83
061	2311366	-3.342	-77.411	013923	015155	FERU/ECUADOR	5.5	33
062	3001257	-60.063	-26.916	222942	224229	S. SANDWICH	6.2	48
063	0102587	-0.114	-17.789	066601	070152	N. ASCENSION	5.5	10
064	2302587	-54.922	-25.350	024339	025517	S. SANDWICH	5.9	27
065	0605387	-0.220	-77.600	041730	043323	ECUADOR	6.5	10
066	0104587	-22.767	-66.205	014808	015951	ARGENTINA	6.1	2499
067	0304587	49.928	78.829	011708	012519	E. KAZAKSTAN	6.2	0
065	2504587	16.066	120.301	121652	123517	PHILIPINE	6.3	104
069	1803587	25.271	94.202	015351	020611	EURMA\INDIA	5.7	50
070	1805587	49.282	147.653	030734	032505	OKHISA SEA	6.1	542
071	2006587	49.913	78.735	005304	010416	E. KAZAHKST	6.1	0
072	1706687	-5.755	130.791	013259	015144	BANDA SEA	6.6	67
073	2806587	32.820	24.357	245017	245555	COAST OF Libya	5.2	24

074	061087	-17.940	-172.225	041906	043916	TONGA IS.	6.2	40
075	081087	-19.599	-173.111	032045	034051	TONGA IS.	6.7	16
076	161087	-6.266	149.060	204801	210725	NEW BRITAIN	5.9	48
077	251087	5.409	36.751	164813	165300	ETHIOPIA	5.6	12
078	271087	-3.850	139.450	220147	220921	WEST IRIAN	5.0	33
079	271087	-28.676	-62.929	215817	220920	ARGENTINA	6.0	605
080	301187	58.676	-142.786	192319	194100	GULF OF ALASKA	6.7	10
081	070188	0.549	18.442	225554	230340	ZAIRE	4.8	33
082	130188	-4.649	153.147	162313	164247	IRELAND	5.8	29
083	060388	56.953	-143.032	223538	225500	GULF OF AL.	6.8	10
084	090388	-17.327	-74.154	213353	214631	PERU	6.0	32
085	090388	57.069	-142.905	040203	041255	GULF OF AL.	-	10
086	100388	10.402	-60.587	061723	062311	TRINIDAD	6.2	56
087	120388	10.144	-60.569	043210	044300	TRINIDAD	5.7	52
088	210388	77.601	125.451	233121	235355	LAPTEV SEA	6.0	10
089	250388	-32.241	-14.728	041943	042724	S. ATLANTIC	5.0	10
090	260388	33.280	13.280	120729	121900	MEDITERRANIAN	4.7	10
091	280388	19.966	-156.449	035833	045320	HAWAII	5.2	46
092	300388	-24.925	-70.461	230556	240332	N. COAST OF N. CHILE	5.8	41
093	030488	-30.802	117.086	243959	245422	W. AUSRALIA	-	10
094	120488	-17.192	-72.305	231955	233225	NEAR COAST OF PERU	6.1	33
095	040588	49.928	78.769	005706	010817	E. KAZAKH	5.4	0
096	070588	-0.467	30.006	050533	051800	UGANDA	4.5	10
097	050788	-5.964	148.760	203207	205125	NEW BRITAIN	6.0	53
098	230788	-6.526	152.779	151708	153645	NEW BRITAIN	6.7	17
099	250788	-6.081	133.667	064615	070509	ARCE ISLAND	6.5	28
100	270788	-13.112	167.051	215509	221450	VANUATU IS.	5.9	172
101	300788	-15.230	-173.440	004957	011004	TONGA IS.	5.0	33
102	060888	25.149	95.127	243624	244844	BURMA/INDIA	6.8	91
103	060888	-7.136	151.057	062655	064630	NEW BRITAIN	5.9	25
104	060888	35.461	71.043	090321	091323	AFGANISTAN	6.1	195
105	100888	-10.366	160.819	043826	045828	SOLOMON IS.	6.1	34
106	140888	-27.260	-71.092	175309	180542	N. C. OF CHILE	5.7	33
107	200988	26.755	86.616	230909	232057	NEPAT	6.4	57
108	140988	49.833	78.808	035957	041108	E. KAZAKH	6.1	0
109	140988	-23.424	-67.997	221407	222614	CHILE/ARGENTINA	5.7	123
110	150988	-1.442	-77.866	184601	190023	ECUADOR	5.8	170
111	161088	37.938	20.932	123405	124010	IONIAN SEA	5.5	25
112	311088	36.443	2.759	101258	102643	ALGERIA	5.4	12

113	051188	34.354	91.880	021430	022638	QINAHAI	5.9	08
114	061188	22.789	99.611	130319	131611	BURMA/CHINA	6.1	18
115	061188	23.181	99.439	131543	132834	BURMA/CHINA	6.1	10
116	061188	23.029	99.789	202424	203716	BURMA/CHINA	5.4	10
117	071188	-22.239	175.018	035000	041005	S. OF FRANCE	5.7	22
118	141188	-3.527	150.120	021539	023510	IRELAND	5.9	33
120	181188	-6.125	149.785	193854	195822	NEW BRITAIN	5.8	61
121	201188	35.281	28.685	210105	210724	E. MEDITERRANIAN	-	10
122	251188	48.117	-71.183	234604	235741	S. QUEBEC	5.9	29
123	041288	73.387	54.998	051953	053054	NOVAYA	5.5	0
124	061288	-1.457	-15.244	194231	194807	N. OF ASCENSION	5.3	10
125	071288	40.987	44.185	074124	074930	TURKEY	6.2	05
126	131288	71.134	-7.634	040138	041152	JAM MAYAEM;	5.7	10
127	241288	-23.522	-66.666	042654	043848	JUJUY PROVINCE	5.7	197
128	020189	-18.589	-174.559	015208	021206	TONGA IS.	6.1	108
129	030189	35.626	11.630	165219	170500	TUNISIA	5.0	10
130	030189	4.441	95.061	170033	170500	N. SUMATERA	5.0	10
131	060189	35.592	11.694	052658	053022	TUNISIA	5.1	08
132	220189	49.924	78.831	035705	040817	E. KAZAKH	6.1	0
133	040289	0.082	-16.658	155152	155732	N. OF ASCENSION	5.6	10
134	040289	-4.625	153.066	221038	223013	NEW IRELAND	6.1	52
135	090289	-8.548	29.836	234916	235300	L. TANGAYIKA	5.2	35
136	120289	39.136	27.660	121332	121600	TURKEY	5.4	10
137	250289	-29.915	-177.985	112635	114634	KARMADEC IS.	6.1	31
138	050489	-20.857	-69.028	234749	235957	NORTHERN CHILE	5.7	112
139	060489	-19.306	169.002	080557	081744	VANUATU IS.	6.1	166
140	110489	35.860	81.230	135008	140146	XINJIAN	5.1	33
141	150489	39.403	28.332	040816	041515	TURKEY	-	10
142	250489	30.048	99.419	021320	022605	SICHUAN IS.	6.2	08
143	300489	10.960	-68.325	082254	083432	COAST OF VENEZUELA	5.9	30
144	030589	30.091	99.475	055301	060544	SCHUAN PROVINCE	6.1	14
145	050589	-8.281	-71.381	182835	183951	WESTERN BRAZIL	6.1	593
146	080589	-23.427	-179.853	142839	143739	SOUTH OF FIJI	5.6	548
147	140589	-30.523	-178.414	005950	011946	KARMADEC IS.	5.9	44
148	150589	45.472	151.693	212353	214951	KURILE ISLAND	5.3	33
149	230589	-52.341	160.568	105446	111405	MACQUARIE	6.4	10
150	090789	-1.577	-15.548	094637	095214	NORTH ASCENSION	5.4	10
151	140789	-1.472	-15.546	154318	154857	NORTH ASCENSION	5.4	10
152	220789	2.299	128.142	050211	052047	HALMATTERA	6.4	142

153	240789	36.085	71.069	032748	033800	AFGANISTAN	5.8	95	
154	210689	-4.104	154.459	182541	184429	SOLOMON IS.	5.8	494	
155	090989	2.435	-79.761	014035	015323	S. OF PANAMA	6.0	07	
156	160989	40.337	51.534	020508	021346	CASPIAN SEA	6.4	55	
157	170989	40.203	51.749	005339	010219	CASPIAN SEA	6.1	51	
158	220989	31.583	102.433	022550	023644	SICHUAN PROVINCE	6.1	15	
159	271089	-11.022	162.352	210451	212445	SOLOMON IS.	6.1	25	
160	151189	-0.584	-19.985	040040	040651	C. MID ATLANTIC	5.5	10	
161	191189	-11.343	118.021	035713	040910	SOUTH OF SUMB	5.3	25	
162	291189	-15.808	-73.242	010014	011240	SOUTHERN PERU	6.1	71	
163	040190	-15.397	-172.850	053221	055227	SAMOA ISLAND	6.4	54	
164	090190	24.753	95.241	185129	190345	BURMA	6.1	119	
165	100190	39.706	143.306	030918	031524	E. COAST JAPAN	5.7	37	
166	130390	-3.994	39.625	230529	232357	KENYA	5.3	10	
167	150390	-15.130	167.238	045634	051622	VANUATU IS.	5.6	132	
168	210390	-31.092	-179.093	164605	170548	KARMADEC IS.	6.2	145	
169	260490	36.239	100.254	093745	094940	china	6.3	10	
170	020590	-5.604	150.164	225029	230952	NEW BRITAIN	6.2	82	
171	140590	-35.925	-71.415	213404	214648	CENTRAL CHILE	5.8	76	
172	150590	36.043	70.428	142520	143528	HINDU KUSH	5.9	113	
173	150590	-3.225	35.744	152126	153740	TANZANIA	5.9	05	
174	150590	-3.075	35.891	162419	164035	TANZANIA	5.5	05	
175	190590	25.517	91.063	021855	022728	INDIA/BANG	-	33	
176	240590	5.356	31.848	200006	200530	SUDAN	6.5	16	
177	240590	5.436	31.876	221603	222757	SUDAN	5.5	10	
178	250590	5.425	31.848	244231	245529	SUDAN	5.3	10	
179	260590	5.134	31.769	142240	143539	SUDAN	5.0	10	
180	300590	45.841	25.668	104006	104520	ROMANIA	6.7	89	
181	310590	45.811	28.769	241747	242500	ROMANIA	6.1	83	
182	030690	5.442	32.121	162329	163630	SUDAN	5.1	10	
183	090690	5.445	32.022	080603	081900	SUDAN	4.7	10	
184	170690	27.398	65.719	045145	050131	PAKISTAN	5.9	15	
185	200690	36.957	49.409	210009	210935	W. IRAN	6.1	19	
186	200690	5.412	31.717	184758	190100	SUDAN	5.0	16	
187	090790	5.395	31.654	151120	151635	SUDAN	5.9	13	
188	140790	0.003	-17.376	055425	060009	N. ASCENSION	6.2	11	
189	270790	-15.355	167.464	123759	125745	VANUATU;IS.	6.4	126	
190	280790	5.225	32.604	164602	165846	SUDAN	5.3	10	
191	160790	-32.460	69.958	145148	150405	N. ITALY	5.7	102	

192	050890	-1.080	-13.887	174232	174754	N. ASCENSION	5.6	10	
193	040990	-0.479	29.085	014800	015323	ZAIRE	5.0	10	
194	070990	5.443	31.686	241226	242518	SUDAN	5.2	33	
195	121290	16.590	-97.190	241945	243010	MEXICO	5.2	10	
196	151290	0.180	29.529	205651	210926	ZAIRE	4.7	18	
197	280191	30.570	129.010	180925	182034	JAPAN	5.6	33	
198	110391	-51.154	29.255	211556	212635	S. AFRICA	5.8	10	
199	120791	-39.368	175.902	044223	050208	N. ZEALAND	5.3	67	
200	200791	16.891	-99.479	155250	161100	MEXICO	-	10	
201	230791	36.547	140.589	145347	155700	JAPAN	4.9	112	
202	280991	-5.814	150.959	202656	204628	NEW BRITAIN	5.8	28	
203	261191	42.051	142.523	194048	200007	JAPAN	6.1	56	
204	201291	24.720	93.103	020605	021833	MYANMA/INDIA	5.3	41	
205	251291	45.667	151.734	192323	192350	KURIL IS.	5.4	29	
206	251291	21.442	144.325	185745	192350	MARIANA IS.	5.1	33	
207	130292	-15.894	166.318	012913	014915	VANUATU IS.	6.1	10	
208	260292	11.803	57.764	034519	035410	ARABIAN SEA	5.8	10	
209	030492	35.404	-118.480	030803	030924	C. CALIFONIA	-	05	
210	130492	51.153	5.798	012000	012731	NETHERLANDS	5.5	21	
211	210592	41.604	88.813	045957	051147	CHINA	6.5	0	
212	060892	42.264	21.968	145832	151226	BALKAN REGION	-	10	
213	300892	-17.918	-178.710	200905	202811	FIJI ISLAND	5.8	565	
214	310892	38.310	15.800	242932	245647	SILICY	-	10	
215	150992	-14.053	167.269	210359	212339	VANUATU IS.	6.3	184	
216	190992	29.007	129.320	031958	044549	RYUKYU IS.	4.9	33	
217	230992	-6.163	26.718	145227	150432	ZAIRE	5.6	11	
218	021092	39.735	27.771	241612	244207	TURKEY	5.2	10	
219	051092	15.357	-46.011	015147	020100	N. MID ATLANTIC	5.0	10	
220	071092	54.564	-161.045	154426	161200	ALASKA PENNISULA	5.0	33	
221	071092	10.350	-59.950	222436	223134	N. ATLANTIC OCEAN	-	90	
222	111092	35.995	-117.872	035754	043324	C . CALIFONIA	5.3	03	
223	051192	39.020	27.610	151026	152016	TURKEY	5.2	10	
224	051192	-5.253	152.575	195322	201300	NEW BRITAIN	5.9	20	
225	081192	38.072	27.050	035428	040333	TURKEY	5.8	10	
226	121192	-22.401	-178.104	222857	224823	S. OF FIJI	5.9	360	
227	121192	36.446	70.852	204104	205104	HINDU KUSH	5.7	198	
228	211192	35.916	22.491	050721	051306	C. MEDITTERANIAN	5.9	65	
229	121292	-8.480	121.896	052926	054808	INDONESIA	6.5	28	
230	231292	-15.293	-173.128	243413	245424	TONGA IS	5.9	23	

APPENDIX . II: LIST OF EVENTS WITH ABSOLUTE RESIDUALS ≤ 5.0 S

S/no	DATE	LAT (DEG)	LONG (DEG)	OR. TIME (H. M. S)	ARR. TIME (H. M. S)	REGION	BACKAZ (DEG)	DIST (KM)	DIST (DEG)	J.B TR. TIME (S)	TR. TM. (SEC)	RESIDUAL	MAG	DEPTH (KM)
1.	10 01 85	10.797	-43.446	17 47 56.0	17 56 52	North Atlantic	247.79	5576.3	50.11	537.0	536.5	0.5	5.8	10
2.	18 01 85	-29.374	-70.793	15 00 09	15 12 39	Central Chile	239.07	9518.1	85.54	750.0	746.2	3.8	5.7	83
3.	26 01 85	-33.053	-68.467	03 06 57	03 19 34	Argentina	234.97	9417.2	84.64	757.0	755.9	1.1	6.0	05
4.	31 01 85	-46.063	165.092	04 32 57	04 52 24	Off West Coast of	155.32	15597.6	141.24	1171.0	1169.3	1.7	5.8	10
5.	10 02 85	49.877	78.816	03 27 07	03 38 19	E. Kazakh	40.85	7720.1	69.42	672.0	671.8	0.2	5.9	0
6.	27 02 85	-1.316	-14.568	22 57 40	23 03 07	N. Coast of C. Chile	242.10	2819.7	25.33	328.0	328.5	0.5	4.9	10
7.	05 03 85	35.547	1.438	15 37 55	15 43 21	Algeria	347.91	2774.1	24.94	326.0	325.4	0.6	5.0	10
8.	19 03 85	-33.198	-71.653	04 01 08	04 13 50	N. Coas of C. Chile	235.57	9707.6	87.25	762.0	759.4	2.6	5.9	42
9.	21 03 85	56.523	-34.404	23 54 40	24 04 16	North Atlantic	333.29	6191.6	55.69	576.0	578.9	-2.9	5.1	10
10.	13 04 85	1.622	126.411	03 00 06	03 18 48	Molucca Passage	82.20	13314.3	117.81	1122.0	1122.1	-0.1	6.4	51
11.	20 04 85	9.004	-77.460	18 23 48	18 36 12	North Colombia	277.89	9299.5	83.54	744.0	741.6	2.4	5.6	38
12.	25 04 85	49.924	78.969	00 57 06	01 08 17	East Kaza'stan	40.81	7731.6	69.52	671.0	672.5	-1.5	5.9	0
13.	30 04 85	39.266	22.810	18 14 12	18 20 31	Greece	23.15	3457.4	31.09	379.0	377.5	1.5	5.5	27
14.	06 05 85	-37.498	179.452	17 10 02	17 29 52	E.N. Zealand	165.65	16992.9	152.75	1190.0	1186.5	3.5	5.8	30
15.	10 05 85	-5.599	151.045	15 35 50	15 25 27	New Britain	84.38	15961.1	143.39	1174.0	1172.0	2.0	6.3	27
16.	06 06 85	-4.649	153.173	23 04 55	23 24 28	New Irean	82.04	16171.2	145.26	1172.0	1166.0	5.0	5.6	68
17.	06 06 85	0.932	-28.432	02 40 12	02 47 28	C. Mid-Atlantic	256.68	4145.7	37.24	436.0	434.6	1.4	6.3	10
18.	29 07 85	36.190	70.896	07 54 44	08 04 52	Himdu Kush	54.94	6[illegible]1	61.94	608.0	608.0	0.0	6.6	99
19.	02 08 85	36.174	70.780	07 46 53	07 57 00	Himdu Kush	54.94	6880.5	61.85	607.0	605.2	1.8	6.1	120

20	07 11 85	-35.257	-779.347	19 12 31	19 32 17	E. N. Zealand	166.26	17263.6	155.17	1186.0	1189.1	-3.1	6.2	44
21	16 11 85	-38.577	78.368	04 12 18	04 24 46	Mid-Indian Rise	131.70	9150.6	82.26	746.0	743.0	3.0	5.8	10
22.	14 04 86	-13.923	166.831	00 11 30	00 45 10	Vanuatu Island	99.90	17752.1	159.49	1198.0	1195.5	2.5	6.0	29
23.	24 06 86	-4.446	143.943	03 11 30	03 30 34	New Guinea	64.67	15164.0	136.22	1144.0	1145.8	-1.8	6.6	102
24	13 09 86	37.014	22.196	17 24 31	17 30 32	South Greece	24.55	3213.5	28.89	361.0	361.0	0.0	-	11
25	18 09 86	19.376	146.347	18 20 17	18 39 23	Mariana Region	53.57	14384.1	129.24	1146.0	1148.8	-2.8	5.8	10
26	17 09 86	10.497	56.983	21 25 15	21 34 00	Cariseberg	85.82	5388.6	48.41	525.0	520.9	4.1	4.6	33
27	26 10 86	-5.690	154.051	00 59 23	01 19 01	Solomon Island	83.50	16269.4	146.34	1178.0	1175.6	2.4	5.6	49
28	29 03 86	38.680	25.165	18 36 37	18 43 00	Eagean Sea	27.07	3483.1	31.31	383.0	382.6	0.4	-	10
29	30 01 87	-60.063	-26.916	22 29 42	22 41 29	S. Sandwich	197.04	8468.0	76.17	697.0	701.9	-4.0	6.2	48
30	01 02 87	-0.114	-17.769	06 56 01	07 01 52	N. Ascension	247.79	3077.8	27.25	351.0	349.9	1.1	5.5	10
31	01 04 87	-22.767	-66.205	01 48 08	01 59 51	Argentina	244.29	8875.7	79.75	703.0	701.7	1.3	6.1	249
32	03 04 87	49.928	78.829	01 17 08	01 28 19	E. Kazastan	40.79	7721.7	69.43	671.0	671.9	-0.9	6.2	0
33	18 05 87	25.271	94.202	01 53 52	02 06 11	Burma/India	65.80	9151.6	82.24	740.0	737.3	2.7	5.7	50
34	18 05 87	49.282	147.693	03 07 34	03 25 05	Okhtsa Sea	26.65	12269.4	110.33	1051.0	1047.6	3.4	6.1	542
35	20 06 87	49.913	78.735	00 53 04	01 04 16	E. Kaza'stan	40.80	7714.8	69.37	672.0	672.5	-0.5	6.1	0
36	17 06 87	-5.755	130.79s1	01 32 53	01 51 --	Banda Sea	89.54	13755.0	123.57	1131.0	1126.4	4.6	6.6	67
37	28 06 87	2.820	24.357	0. 50 17	00 55 55	Coast of Libya	32.88	2945.8	26.48	338.0	337.3	0.7	5.2	24
38	06 10 87	-17.940	-172.225	04 19 06	04 39 16	Tonga Island	180.98	19262.5	173.25	1210.0	1208.3	1.7	6.7	16
39	08 10 87	-19.599	-173.111	03 20 45	03 40 51	Tonga Island	175.08	19094.7	171.57	1206.0	1205.0	1.0	6.2	40
40.	16 10 87	-6.266	149.060	20 48 01	21 07 25	New Britain	86.04	15758.5	141.57	1164.0	1160.1	3.9	4.5	59

41.	27 10 87	-28.676	-62.929	21 58 17	22 09 20	Agentina	237.66	8763.7	78.76	663.0	660.3	2.7	6.0	605
42.	13 01 88	-4.649	153.147	16 23 13	16 42 47	Ireland	82.06	16167.5	145.24	1174.0	1175.0	-1.0	5.8	29
43.	09 03 88	-17.327	-74.154	21 33 53	21 46 31	Peru	251.48	9527.5	85.60	758.0	756.4	1.6	6.0	32
44.	12 03 88	10.144	-60.569	04 32 10	04 43 00	Trinidad	276.34	7448.5	66.92	650.0	646.0	4.0	5.7	52
45.	12 04 88	-17.192	-72.305	23 19 55	23 32 25	N. Coast of Peru	251.21	9332.7	83.85	750.0	748.0	2.0	6.1	33
46.	04 05 88	49.928	78.769	00 57 06	01 08 17	E. Kazakhstan	40.79	7717.4	69.40	671.0	671.4	-0.4	5.4	0
47.	23 07 88	-6.526	152.799	15 17 08	15 36 45	New Britain	85.39	16168.6	145.25	1177.0	1176.9	0.1	6.7	17
48.	25 07 88	-6.081	133.667	06 46 05	07 05 09	Arce Island	89.35	14075.0	126.44	1143.0	1140.6	2.4	6.5	26
49.	30 07 88	-15.230	-173.440	00 49 57	01 10 04	Tonga Island	165.40	19568.0	175.81	1207.0	1206.3	0.7	4.9	33
50.	06 08 88	25.149	95.127	00 36 24	00 46 44	Burma/India	65.79	9245.8	83.08	739.0	736.3	2.7	6.8	91
51.	06 08 88	-7.136	151.057	06 26 55	06 46 30	New Britain	86.91	15992.1	143.67	1175.0	1172.8	2.2	5.9	25
52.	06 08 88	36.461	71.043	09 03 21	09 13 23	Afganistan	54.65	6907.8	62.09	602.0	598.5	3.5	6.1	195
53.	14 08 88	-27.260	-71.092	17 53 09	18 05 42	N. Coast of Chile	241.17	9485.5	85.24	755.0	754.5	0.5	5.7	33
54.	14 09 88	49.833	78.809	03 59 57	04 11 08	E. Kazashitan	40.89	7718.9	69.41	671.0	671.8	-0.8	6.1	0
55.	16 10 88	37.938	20.932	12 34 05	12 40 10	Ionian Sea	21.85	3249.6	29.21	365.0	362.4	2.6	5.5	25
56.	05 11 88	34.354	91.880	02 14 30	02 26 38	Qinahai	56.96	8797.2	79.07	728.0	726.1	1.9	5.9	08
57.	06 11 88	22.789	99.611	13 03 19	13 16 11	Burma/India	67.40	9741.3	87.53	772.0	768.0	4.0	6.1	16
58.	06 11 88	23.161	99.439	13 15 43	13 28 34	Burma/India	67.04	9715.7	87.30	771.0	768.2	2.8	6.1	10
59.	06 11 88	23.029	99.789	20 24 2	20 37 16	Burma/India	67.13	9734.1	87.65	772.0	769.6	2.4	5.4	10
60.	07 11 88	-22.239	175.018	03 50 00	04 10 05	S. Of France	133.98	18211.6	163.64	1203.0	1200.0	3.0	5.7	22
61.	14 11 88	-3.527	150.120	02 15 39	02 35 10	Ireland	81.39	15812.0	142.05	1171.0	1174.0	-3.0	5.9	33

62.	20 11 88	35.281	28.685	21 01 05	21 07 25	E. Meditteranian	35.11	3414.9	30.69	378.0	377.0	1.0	-	10
63.	25 11 88	48.117	-71.183	23 46 04	23 57 41	S. Quebec	316.94	8267.6	74.34	697.0	696.6	0.4	5.9	29
64.	04 12 88	73.387	54.998	05 19 53	05 30 54	Novaya	13.19	7553.1	67.96	661.0	663.1	-2.1	5.9	0
65.	06 12 88	-1.457	-15.244	19 42 31	19 48 07	N. of Ascensn	242.59	2892.8	25.99	336.0	334.8	1.2	5.3	10
66.	07 12 88	40.987	44.185	07 41 24	07 49 30	Turkey	40.68	4985.3	43.94	486.0	488.0	-2.0	6.2	05
67.	13 12 88	71.134	-7.634	04 01 38	04 11 52	Jam Mayeam	354.35	6845.0	60.68	614.0	613.8	0.2	5.7	10
68.	22 01 89	49.924	78.831	03 57 06	04 08 17	E. Kazakh	40.80	7721.8	69.44	671.0	672.0	-1.0	6.1	0
69.	04 02 89	0.082	-16.658	15 51 52	15 57 32	N. of Ascensn	247.13	2954.5	26.54	340.0	339.8	0.2	5.6	10
70.	25 02 89	-29.915	-177.685	11 26 35	11 46 34	Kermadecis	165.37	17873.3	160.63	1199.0	1196.0	3.0	6.1	31
71.	05 04 89	-20.857	-69.028	23 47 49	23 59 57	N. Chile	246.87	9098.7	81.75	728.0	727.4	0.6	5.7	112
72.	11 04 89	35.860	81.230	13 50 08	14 01 46	Xinjian	55.87	7618.7	70.28	698.0	701.9	-3.9	4.1	33
73	25 04 89	30.048	99.419	02 13 20	02 26 05	Sichuan Is	60.31	9570.8	86.01	764.0	762.2	1.8	6.2	08
74..	30 04 89	10.960	-68.325	08 22 54	08 34 32	Coast of Venezuel	278.34	8275.8	74.35	698.0	695.5	2.5	5.9	30
75.	03 05 89	30.091	99.475	05 53 01	06 05 44	Sichuan Province	60.26	9575.2	86.05	762.0	761.7	0.3	6.1	14
76.	05 05 89	-8.281	-71.381	18 28 35	18 39 51	Western Brazil	259.70	9011.1	80.95	676.0	674.5	1.5	6.1	593
77.	14 05 89	-30.523	-178.414	00 59 50	01 19 46	Karmadec Is	164 .0	17793.6	159.92	1196.0	1195.2	0.8	5.9	44
78.	23 05 89	-52.341	160.568	10 54 46	11 14 05	Macquarrie	157.37	14840.2	133.46	1159.0	1157.7	1.	6.4	10
79.	09 07 89	-1.577	-15.548	09 46 37	09 52 14	N. of Ascension	242.69	2928.8	26.31	337.0	337.6	-0.6	5.4	10
80.	14 07 89	-1.472	-15.546	15 43 18	15 49 57	N. of Ascension	242.89	2822.9	26.26	339.0	338.9	0.1	5.4	10
81.	24 07 89	36.085	71.069	03 27 48	03 38 00	Afganistan	55.07	6905.3	62.07	612.0.	608.8	3.2	5.8	95
82.	09 09 89	2.435	-79.761	01 40 35	01 53 23	S. of Panama	271.88	9684.6	87.00	768.0	767.3	0.7	6.0	07

83.	16 09 89	40.337	51.534	02 05 08	02 13 46	Caspian Sea	45.16	5378.4	48.35	518.0	514.6	3.4	6.4	55
84.	17 09 89	40.203	51.749	00 53 39	01 02 19	Caspian Sea	45.14	5389.0	48.44	520.0	515.0	5.0	6.1	15
85.	22 09 89	31.583	102.433	02 25 50	02 38 44	Sichuan Pro.	58.31	9820.4	88.26	774.0	772.0	2.0	6.1	25
86.	27 10 89	-11.022	162.352	21 04 51	21 24 45	Solomon Is	92.14	17272.1	155.17	1194.0	1190.0	4.0	6.1	10
87.	15 11 89	-0.584	-19.985	04 00 40	04 06 51	C.Mid-Atlantic	248.78	3322.0	29.84	371.0	369.6	1.0	5.5	71
88.	29 11 89	-15.808	-73.242	01 00 14	01 12 40	Southern Peru	252.76	9394.7	84.41	746.0	745.8	0.2	6.1	37
89.	15 03 90	-15.130	167.238	04 56 35	05 16 22	Vanuatu Is	103.46	17778.8	159.73	1198.0	1195.1	2.9	5.7	145
90	21 03 90	-31.092	-179.093	16 46 05	17 05 48	Karmade Is	163.52	17713.0	159.19	1183.0	1186.5	-3.5	6.2	76
91.	14 05 90	-35.925	-71.415	21 34 04	21 46 48	Central Chile	232.69	9765.3	87.78	764.0	759.3	4.7	5.8	16
92.	24 05 90	5.356	31.848	20 00 09	20 05 30	Sudan	101.56	2740.0	44.61	322.0	320.7	1.3	6.5	89
93.	31 05 90	45.611	28.769	00 17 47	00 25 00	Romania	23.63	43332.7	38.96	433.	438.1	-5.1	6.1	15
94.	17 06 90	27.398	65.719	04 51 45	05 01 31	Pakistan	64.56	6306.0	56.67	566.0	565.2	0.8	5.9	16
95.	09 07 90	5.395	31.654	15 11 20	15 16 35	Sudan	101.60	2718.1	24.42	315.0	318.9	-3.9	5.0	11
96.	14 07 90	0.003	-17.376	05 54 25	06 00 09	N. of Ascension	247.64	3033.6	27.23	344.0	345.9	-1.9	6.2	126
97.	27 07 90	-15.355	167.464	12 37 59	12 57 47	Vanuatu Is	104.20	17798.8	159.91	1186.0	1187.4	-1.4	6.4	10
98.	05 08 90	-1.080	-13.887	17 42 32	17 47 54	N. of Ascension	241.77	2741.0	24.62	322.0	321.7	0.3	5.6	10
99	04 09 90	-0.479	29.085	01 48 00	01 49 00	Zaire	177.10	2637.5	24.23	320.0	317.9	5.1	5.0	10
100.	11 03 91	-51.154	29.255	21 15 56	21 15 56	S. Africa	165.16	7208.6	64.[illegible]	639.0	641.3	-2.3	5.8	10
101.	13 02 92	-15.864	166.318	01 29 13	01 29 13	Vanuatu	105.16	17667.3	158.73	122.0	1197.7	4.3	6.1	10
102.	26 02 92	11.803	57.564	03 45 19	03 45 19	Arabia Is	64.01	5460.3	49.06	531.0	528.8	2.2	5.8	10
103.	13 04 92	51.153	5.798	01 20 00	01 20 00	Nether Lands	358.18	4438.9	39.92	451.0	455.0	-4.0	5.5	21

104.	21 05 92	41.604	88.813	04 59 59	05 11 47	China	49.77	8465.1	76.10	710.0	710.7	-0.7	6.5	0
105	05 10 92	15.357	-49.011	01 51 47	02 01 00	N. Mid-atlantic	280.81	5821.1	52.30	533.0	554.0	-1.0	5.0	10
106.	12 11 92	-22.401	-178.104	22 28 57	22 48 23	S. of Fiji Is	154.53	18644.5	167.3	1166.0	1163.6	2.4	5.9	360
107.	12 11 92	36.446	70.852	20 41 04	20 51 04	Hindu Kush	54.65	6890.5	61.94	600.0	598.5	1.5	5.7	198
108.	12 11 92	35.916	22.491	05 07 21	05 13 06	C. Medilt	26.20	3124.3	28.08	345.0	343.8	1.2	5.9	65
109	12 12 92	-8.480	121.896	05 29 08	05 48 08	Indonesia	94.17	12830.0	115.26	1122.0	1118.5	3.5	6.5	28
110.	23 12 92	-15.283	-173.128	00 34 13	00 54 24	Tonga Is	169.61	19566.6	175.81	1211.0	1208.1	2.9	5.9	23

APPENDIX III: List of events used in Computing relative residuals

Date	Event Region	Dist(D°)	Station Code & country	Absolute station Res R_a	Zaria Station Res R_z	Relative Res. $R_a=R_a-R_z$
270285	North Ascension	25.33	KIC Cote D'Ivore	-5.1	+0.5	-5.6
			KDS Senegal	-4.7		-5.2
			KBC Cameroon	+0.6		+0.1
			BNG C.Africa Republic	-1.0		-1.5
			LWI Zaire	-0.5		+1.0
			NAI Kenya	+1.7		+1.2
061288	North Ascension	25.99	LIC Cote D'Ivoire	-7.3		-8.0
			TIC "	-6.3	+0.7	-7.0
			KIC "	-7.1		-7.8
			LEGH Ghana	-4.2		-4.9
			KUK "	-4.4		-5.1
			KOGH "	-3.8		-4.5
			SHGH "	-3.2		-3.9
			BNG Central Africa	-2.4		-3.1
			LWI Zaire	-0.9		-1.6
040289	North Ascension	26.54	LIC Cote D'Ivoire	-5.1		-5.3
			TIC "	-5.1	+0.2	-5.3
			KIC "	-4.7		-4.9
			KUK Ghana	-3.4		-3.6
			LEGH "	-1.9		-2.1
			KOGH "	-2.4		-2.6
			SHGH "	-1.6		-1.8
			BCAO C.A.R	-0.2		-0.4
			BNG "	+0.5		+0.3
			LWI Zaire	+0.7		+0.5
090789	North Ascension	26.31	LIC Cote D'Ivoire	-5.0		-4.4
			TIC "	-5.3	-0.6	-4.7
			BNG C.A.R	+0.6		+1.2
			LWI Zaire	+0.5		+1.1
140790	North Ascension	27.23	LIC Cote D'Ivoire	-3.9		-2.5
			TIC "	-4.4	-1.4	-3.0
			KIC "	-4.1		-2.7
			BCAO C.A.R	+1.3		+2.7
300485	Greece	31.08	KBC Cameroon	+2.1		0.6
			EKC "	+1.6	+1.5	0.1
			KIC Cote D'Ivoire	-0.8		-2.3
			NAI Kenya	+1.5		0.0

291189	South of Peru	84.41	LIC Cote D'Ivore	-1.6	+0.3	-1.9
			TIC "	-1.4		-1.7
			KIC "	-1.4		-1.7
			KUK Ghana	-0.6		-0.9
			LEGH "	-1.7		-2.0
			SHGH "	-0.9		-1.2
			BCAO C.A.R	-0.4		-0.7
030487	East Kazakhstan	69.43	IIC Cote D'Ivoire	-0.1	-0.4	+0.3
			KIC "	-0.0		+0.4
			LIC "	-0.1		+0.3
			BNG C.A.R	-1.3		-0.9
			BCAO "	-1.2		-0.8
			NAI Kenya	+1.1		+1.5
			LWI Zaire			
			NAI Kenya			
040588	East kaz'stan	69.40	TIC Cote D'Ivoire KIC Cote	-0.2	-1.2	+1.0
			D'Ivoire	-0.1		+1.1
			LIC "	0.1		+1.1
			SHGH Ghana	-0.2		+1.0
			LEGH "	+0.1		+1.3
			LWI Zaire	-0.6		+0.6
200687	East Kaz'stan	69.37	TIC Cote D'Ivoire	0.0	-0.4	+0.4
			KIC "	+0.1		+0.5
			LIC "	0.0		+0.4
			BNG C.A.R	-1.1		-0.7
			LWI Zaire	-0.5		-0.1
			NAI Kenya	-0.6		-0.2
220189	East Kaz'stan	69.44	TIC Cote D'Ivoire	0.0	-1.1	+1.1
			KIC "	+0.1		+1.2
			LIC "	0.0		+1.1
			KUK Ghana	-0.4		+0.7
			SHGH "	-0.4		+0.7
			LEGH "	0.0		+1.1
			BNG C.A.R	-1.0		+0.1
			LWI Zaire	-0.9		+0.2
290386	Eagean Sea	31.31	KIC Cote D'Ivoire	-1.0	+0.4	-1.4
			BNG C.A.R	-1.4		-1.8
			LWI Zaire	-4.9		-5.3
			NAI Kenya	+4.8		+4.4
060888	BURMA-INDIA BOARDER	83.08	KIC Cote D'Ivoire	+0.3	+2.6	-2.3
			TIC "	+0.1		-2.5
			LIC "	-0.1		-2.7
			KUK Ghana	-0.1		-2.7
			KOGH "	+0.2		-2.4
			LEGH "	+0.1		-2.5
			LWI Zaire	+0.3		-2.3

291189	South of Peru	84.41	LIC Cote D'Ivore	-1.6	+0.3	-1.9
			TIC "	-1.4		-1.7
			KIC "	-1.4		-1.7
			KUK Ghana	-0.6		-0.9
			LEGH "	-1.7		-2.0
			SHGH "	-0.9		-1.2
			BCAO C.A.R	-0.4		-0.7
030487	East Kazakhstan	69.43	IIC Cote D'Ivoire	-0.1	-0.4	+0.3
			KIC "	-0.0		+0.4
			LIC "	-0.1		+0.3
			BNG C.A.R	-1.3		-0.9
			BCAO "	-1.2		-0.8
			NAI Kenya	+1.1		+1.5
			LWI Zaire			
			NAI Kenya			
040588	East kaz'stan	69.40	TIC Cote D'Ivoire KIC Cote	-0.2	-1.2	+1.0
			D'Ivoire	-0.1		+1.1
			LIC "	0.1		+1.1
			SHGH Ghana	-0.2		+1.0
			LEGH "	+0.1		+1.3
			LWI Zaire	-0.6		+0.6
200687	East Kaz'stan	69.37	TIC Cote D'Ivoire	0.0	-0.4	+0.4
			KIC "	+0.1		+0.5
			LIC "	0.0		+0.4
			BNG C.A.R	-1.1		-0.7
			LWI Zaire	-0.5		-0.1
			NAI Kenya	-0.6		-0.2
220189	East Kaz'stan	69.44	TIC Cote D'Ivoire	0.0	-1.1	+1.1
			KIC "	+0.1		+1.2
			LIC "	0.0		+1.1
			KUK Ghana	-0.4		+0.7
			SHGH "	-0.4		+0.7
			LEGH "	0.0		+1.1
			BNG C.A.R	-1.0		+0.1
			LWI Zaire	-0.9		+0.2
290386	Eagean Sea	31.31	KIC Cote D'Ivoire	-1.0	+0.4	-1.4
			BNG C.A.R	-1.4		-1.8
			LWI Zaire	-4.9		-5.3
			NAI Kenya	+4.8		+4.4
060888	BURMA-INDIA BOARDER	83.08	KIC Cote D'Ivoire	+0.3	+2.6	-2.3
			TIC "	+0.1		-2.5
			LIC "	-0.1		-2.7
			KUK Ghana	-0.1		-2.7
			KOGH "	+0.2		-2.4
			LEGH "	+0.1		-2.5
			LWI Zaire	+0.3		-2.3

280687	Coast of Libya	26.48	TIC Cote D'Ivore	-1.5	+2.0	-3.5
			KIC "	-1.6		-3.6
			LIC "	-1.5		-3.5
			KDS Senega	-1.1		-3.1
			BNG Central Afri. R	-2.0		-4.0
			BCAO "	-2.4		-4.4
			LWI Zaire	-1.2		-3.2
			NAI Kenya	+2.6		+0.6
161088	Ionian Sea	29.21	TIC Cote D'Ivoire	-0.9	+2.6	-3.5
			KIC "	-0.8		-3.4
			LIC "	-0.7		-3.3
			KUK Ghana	-1.6		-4.2
			SHGH "	+1.1		-1.5
			LEGH "	-0.3		-2.9
			LWI Zaire	-0.2		-2.8
			NAI Kenya	+1.9		-0.7
201188	East Mediterranian	30.69	TIC Cote D'Ivoire KIC	-0.1	+1.0	-1.1
			Cote D'Ivoire	0.0		-1.0
			LIC "	0.0		-1.0
			KUK Ghana	+0.1		-0.9
			SHGH "	+0.5		-0.5
			LEGH "	+0.6		-0.4
			BNG C.A.R	+1.1		+0.1
			LWI Zaire	+2.4		+1.4
130986	Southern Greece	28.89	TIC Cote D'Ivoire	-0.8	0.0	-0.8
			KIC "	-1.0		-1.0
			LIC "	-3.0		-3.0
			BNG C.A.R	-1.5		-1.5
			BCAO C.A.R	-0.8		-0.8
			LWI Zaire	+0.5		0.5
			NAI Kenya	+3.4	1.1	3.4
260185	Argentina	84.64	LIC Cote D'Ivore	-2.7		-3.8
			TIC "	-2.5		-3.6
			KIC "	-2.6		-3.7
			BCAO C.A.R	-0.8		-1.9.
			BNG "	-1.7		-2.8
			NAI Kenya	+6.2		+5.1

180587	BURMA-INDIA	82.24	KIC Cote D'Ivoire	+0.1	-0.4	+0.5
			LIC "	0.0		+0.4
			TIC "	0.0		+0.4
			BNG Central A. Rep.	-1.1		-0.7
			LWI Zaire	-0.5		-0.1
			NAI Kenya	-0.6		-0.2
250489	Sichman Province China	86.01	TIC Cote D'Ivoire	+0.1	2.8	-2.7
			LIC "	+0.1		-2.7
			KUK Ghana	+1.5		-1.3
			KOGH "	-0.2		-3.0
			BNG C.A.R	-0.7		-3.5
			BCAO "	-0.6		-3.4
			LWI Zaire	-0.4		-3.2
030589	Sichman Province China	86.05	KIC Cote D'Ivoire	0.0	+0.3	-0.3
			TIC "	-0.1		-0.4
			LIC "	-0.2		-0.5
			KUK Ghana	+3.2		+2.9
			KOGH "	+5.5		+5.2
			LEGH "	+4.7		+4.4
			BNG C.A.R	-1.1		-1.4
			BCAO "	-1.0		-1.3
			LWI Zaire	+0.6		+0.3
220989	Sichman Province China	88.26	BNG C.A.R	-0.3	+1.1	-1.4
			BCAO "	-1.1		-2.2
050890	North Coast of Ascension	24.62	LIC Cote D'Ivoire	-6.6	+0.3	-6.9
			NAI Kenya	+2.4		+2.1
120488	Near Coast of Peru	83.86	TIC Cote D'Ivoire	-1.3	2.0	-3.3
			KIC "	-1.3		-3.3
			LIC "	-1.4		-3.4
			LEGH Ghana	-3.1		-5.1
			KUK "	-0.9		-2.9
090989	South of Panama	87.00	LIC Cote D'Ivoire	-0.8	+0.7	-1.5
			TIC "	-1.0		-1.7
			KIC "	-0.9		-1.6
			BNG C.A.R	-0.8		-1.6